

## STRUCTURAL CHEMISTRY OF HEMERYTHRIN

DONALD M. KURTZ, Jr., DUWARD F. SHRIVER and IRVING M. KLOTZ

*Department of Chemistry and Department of Biochemistry and Molecular Biology,  
Northwestern University, Evanston, Illinois 60201 (U.S.A.)*

(Received 15 April 1977)

### CONTENTS

A. Introduction . . . . .	145
B. Physiological properties . . . . .	146
C. Molecular properties . . . . .	147
D. The oxygen binding site . . . . .	149
(i) Electronic spectra . . . . .	152
(ii) Magnetic susceptibility . . . . .	152
(iii) Mössbauer spectra . . . . .	153
(iv) Chemical modification . . . . .	154
(v) X-ray crystallography . . . . .	155
(a) Azidometmyohemerythrin . . . . .	155
(b) Aquomethemerythrin . . . . .	155
(vi) Resonance Raman spectroscopy . . . . .	156
(a) Oxy- and azidomethemerythrin . . . . .	157
(b) Thiocyanatomethemerythrin . . . . .	159
(c) Other complexes of methemerythrin . . . . .	161
(d) Unsymmetrically isotopic ligands . . . . .	161
(e) Oxygen-18 water . . . . .	167
(vii) Models for the oxygen binding site of hemerythrin . . . . .	171
E. Comparison of the oxygen binding sites of hemerythrin and hemoglobin . . . . .	175
References . . . . .	177

### A. INTRODUCTION

The process of respiration in almost all forms of higher animal life involves some means for concentrating molecular oxygen from the environment and for transporting and storing it within the organism. These requirements have been met by the evolution of three alternative classes of proteins which bind oxygen reversibly: the hemoglobins, the hemerythrins, and the hemocyanins. These oxygen transporting proteins occur in high concentrations ( $>10^{-3}$  M) in vivo and are relatively easy to isolate. Because of their obvious physiological importance, these proteins have been studied intensely for at least a century.

Hemoglobins are distributed among most major phyla of the animal king-

TABLE 1

Comparison of some properties of the oxygen binding pigments

	Hemoglobin	Hemerythrin	Hemocyanin
Metal	Fe	Fe	Cu
Metal : O <sub>2</sub>	Fe : O <sub>2</sub>	2Fe : O <sub>2</sub>	2Cu : O <sub>2</sub>
Oxidation state of metal in the deoxy protein	Fe <sup>II</sup>	Fe <sup>II</sup>	Cu <sup>I</sup>
Coordination of metal	Porphyrin	Protein side chains	Protein side chains
No. subunits	4	8	Variable
Mol. wt.	65,000	108,000	400,000—9,000,000
Color			
Oxygenated	Red	Violet-pink	Blue
Deoxygenated	Red-blue	Colorless	Colorless

dom, whereas hemerythrins and hemocyanins are restricted to distinct invertebrate phyla. It is intriguing to try to establish how the three alternative evolutionary paths have adapted different molecular components and structures to perform the same physiological function, namely the transport of oxygen.

Table 1 provides a comparison of some of the properties of these three classes of proteins. Distinctive properties of the invertebrate oxygen carriers hemerythrin and hemocyanin are their binuclear metal centers, their lack of a heme prosthetic group (despite their names), and their relatively large molecular size in vivo. The active center of hemoglobin has probably been more intensively studied than that of any other protein or enzyme. The purpose of this article is to review the recent advances which have been made in the elucidation of the structure and electronic nature of the oxygen binding site of the invertebrate oxygen carrier, hemerythrin. Reviews of the physiological and molecular properties, electronic and Mössbauer spectral properties and magnetic susceptibility studies of hemerythrin have appeared elsewhere [1—4]. This review emphasizes the two most recent advances in hemerythrin chemistry, namely, resonance Raman spectral properties and X-ray crystallographic results. These recent results are combined with the earlier data in an attempt to construct a reasonable picture of the oxygen binding site.

## B. PHYSIOLOGICAL PROPERTIES

The source of hemerythrin that has been used for most of the molecular investigations is a sipunculan worm from the North American Atlantic coast *Phascolopsis* (syn. *Golfingia*) *gouldii*. Hemerythrin occurs in erythrocytes of

the coelomic cavity of these animals. The oxygen affinity of hemerythrin (oxygen pressure at half-saturation,  $P_{50} \sim 3-5$  mm [5,6]) is much stronger than that of hemoglobin ( $P_{50} \sim 20-40$  mm [7]), and values of the Hill coefficient, ranging from 1.2–1.4 [1–5] (compared to the value of 2.8 for hemoglobin [7]) show that hemerythrin binds oxygen with little or no cooperativity. Some coelomic hemerythrins have Bohr effects, while others, including that of *P. gouldii*, are insensitive to pH [1,4]. The differences in physiological properties of hemerythrin compared to hemoglobin can be rationalized in terms of their functions. Hemerythrin occurs in the coelomic cavity of the sipunculids and oxygen is absorbed through the body wall [1,6]. Coelomic hemerythrin is used mainly for oxygen storage and thus does not need to respond to small differences in oxygen tension as it would if, like hemoglobin, it were a part of a vascular network for transport of oxygen.

### C. MOLECULAR PROPERTIES

Hemerythrin isolated from erythrocytes occurs as an octamer of molecular weight near 108 000. It is constituted of eight identical subunits [8] each of which contains two iron atoms. A myohemerythrin isolated from the retractor muscles of sipunculids occurs as a monomer and has a molecular weight corresponding to that of a subunit in the octameric protein [9].

Chemical modification, for example of the cysteine sulfhydryl group [8], will dissociate the octamer into monomers. Figure 1 shows the interconversions between octamer and monomers and between different chemical states of hemerythrin. As shown in Fig. 1, irreversibly oxidized met- and mero-hemerythrins lose their ability to reversibly bind oxygen.

Although Fig. 1 pictures the subunits in a cubic array, recent low resolution X-ray crystallographic studies [10,11] show the correct subunit arrangement to be nearer that of a square antiprism (Fig. 2). The molecule resembles a square doughnut composed of two tetramers which face each other. A square channel, 20 Å on a side, through the middle of the doughnut may provide the easiest access to the iron sites for oxygen and other ligands.

The tertiary structure of the myohemerythrin monomer has been solved at low resolution [12] as have those of *P. gouldii* and of *T. dyscritum* coelomic octameric hemerythrins [10,11]. All of these studies show a structure for the monomer resembling the drawing in Fig. 3. The structure consists of four nearly parallel helical segments, 30–40 Å long, connected by short non-helical turns. The helices embrace the two iron atoms. A non-helical  $\text{NH}_2$ -terminal arm is appended to the left side of the structure. The line connecting the iron atoms is perpendicular to the plane of the page showing Fig. 3. The model indicates that about 75% of the amino acid residues are in helical segments, which agrees quite well with earlier circular dichroism studies [13].

Figure 4 shows two views of the arrangement of the subunits of Fig. 3 in

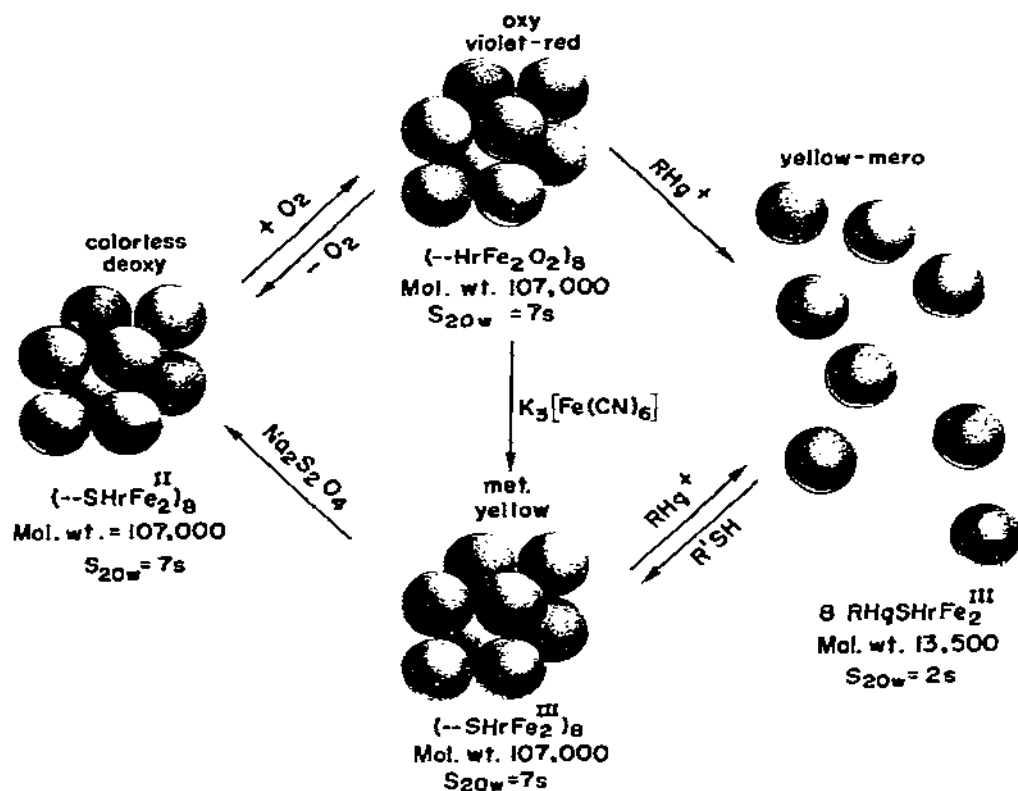


Fig. 1. Macromolecular properties of and interrelationships between deoxy-, oxy- and methemerythrin and their monomeric subunit.

the quaternary structure of hemerythrin [10]. The molecule possesses  $D_4$  symmetry with the fourfold axis  $R$  passing through the central 20 Å channel.

The primary structure of hemerythrin has been established [14] and is shown in Fig. 5. Five genetic variants of *P. gouldii* hemerythrin have been identified [15], and their amino acid substitutions have been useful for reducing the number of possible protein ligands to the irons.

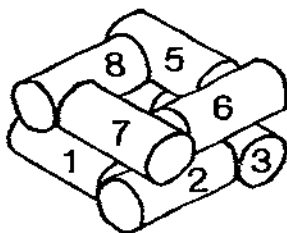


Fig. 2. Schematic drawing of the subunit arrangement of hemerythrin.

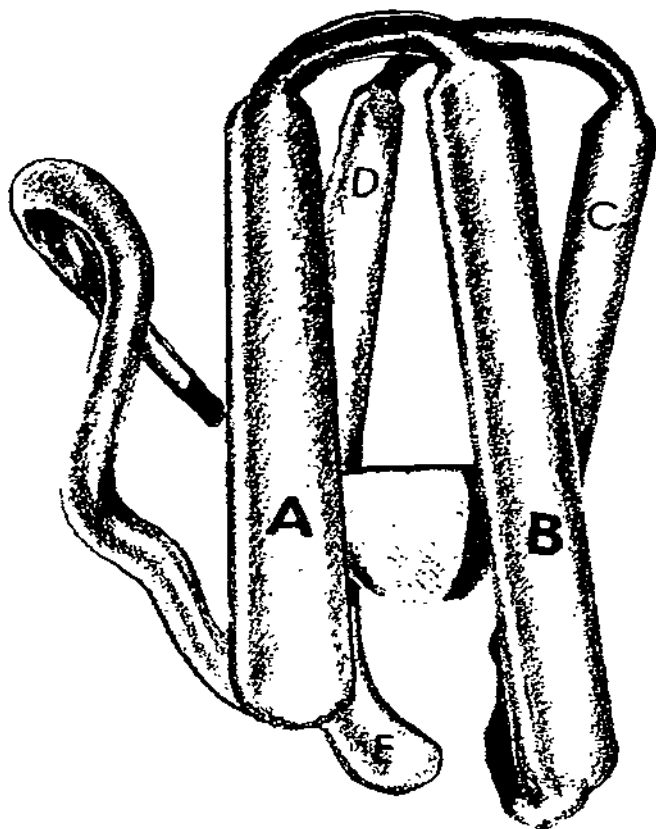
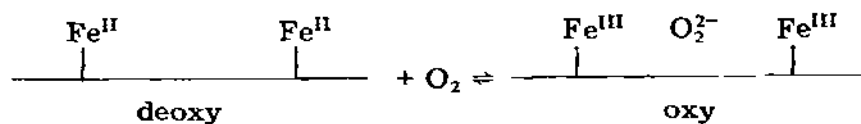


Fig. 3. Molecular model of monomeric myohemerythrin at low resolution. The four approximately parallel helical segments are labeled, A, B, C, and D. The C-terminal helical stub is designated E. Taken from [12] with permission of the authors.

#### D. THE OXYGEN BINDING SITE

The stoichiometry of the oxygen uptake,  $2 \text{ Fe} : 1 \text{ O}_2$  [16,17] suggests that the two iron atoms are in proximity in hemerythrin, with the dioxygen molecule perhaps bridging them. The state of iron in deoxyhemerythrin was established as  $\text{Fe(II)}$  by chemical means [18]. The state of iron in oxyhemerythrin could not be so easily established, but it was suggested [18] that the oxygenation reaction should be formulated as



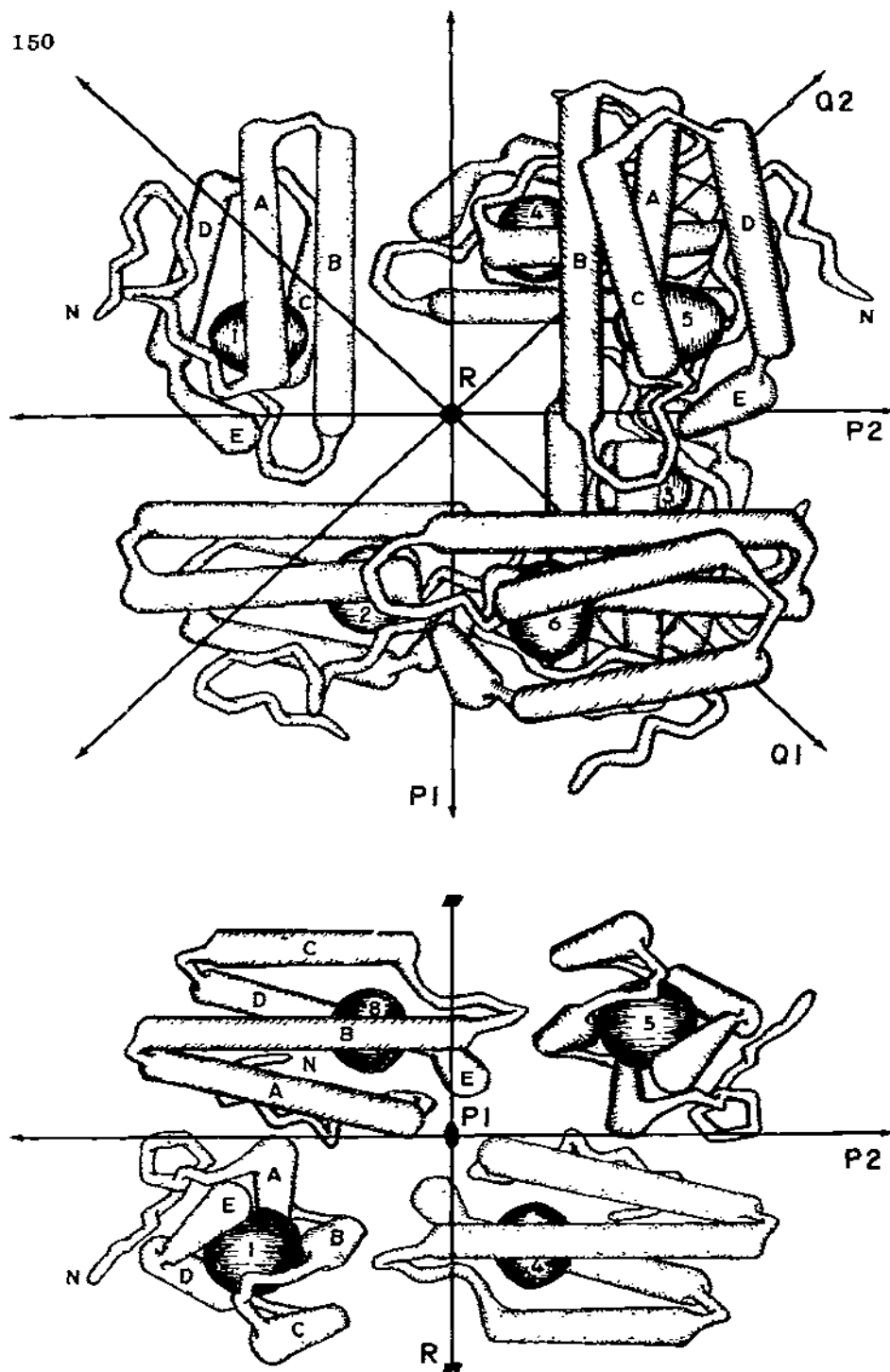


Fig. 4. Two views of the quaternary structure of hemerythrin. Subunit numbering follows Fig. 2. Taken from [10] with permission of the authors.

## HEMERYTHRIN

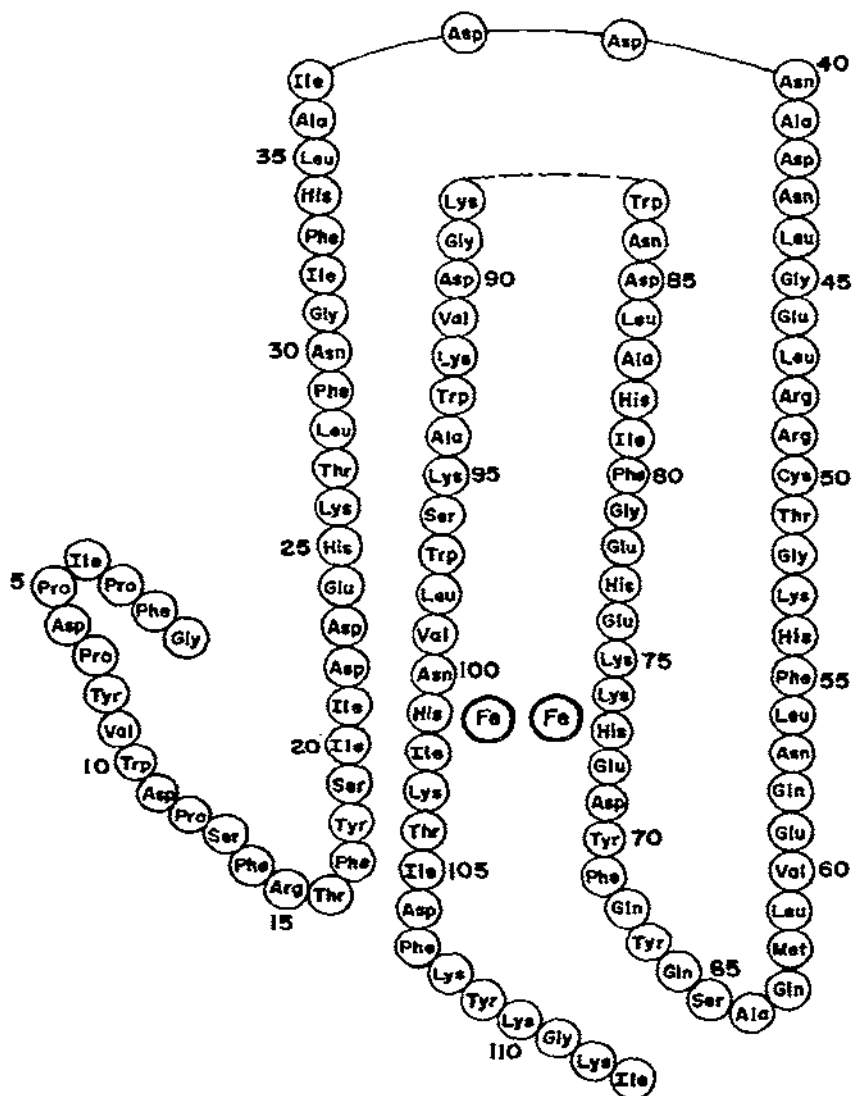


Fig. 5. Primary structure of hemerythrin from erythrocytes of *P. gouldii*.

Hemerythrin has since been examined by a number of physical techniques which have confirmed this early formulation for the changes in oxidation states while revealing additional structural and electronic features of the oxygen-binding site.

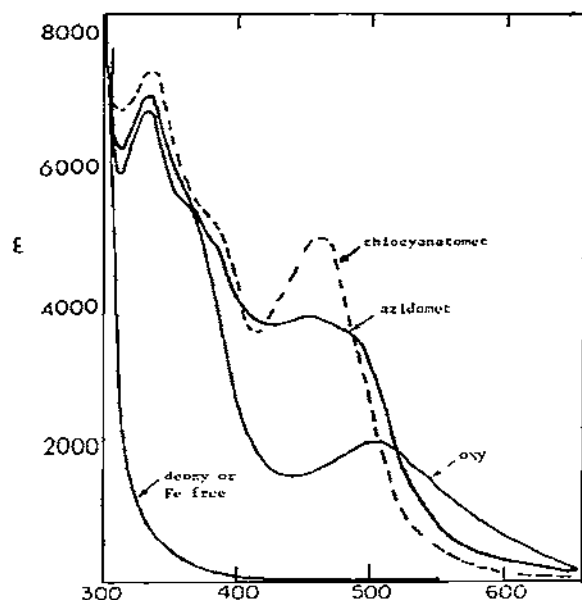


Fig. 6. Visible absorption spectra of deoxy-, oxy-, azidomet- and thiocyanatomethemerythrin.

#### (i) Electronic spectra

Irreversibly oxidized, Fe(III) methemerythrin will combine with several anionic ligands such as chloride, azide, or thiocyanate in the same 2 Fe : 1 ligand stoichiometry [19,20] as does dioxygen. Electronic absorption spectra of these methemerythrin-ligand complexes [3,19] bear close resemblance to that of oxyhemerythrin and suggest similar oxidation states and structures for oxy- and methemerythrins. Figure 6 shows the similarity of absorption spectra of oxy-, azidomet-, and thiocyanatomethemerythrin and their dissimilarity to the spectrum of deoxyhemerythrin. The similarities in ligand  $\rightarrow$  iron charge transfer energies [3] for  $N_3^- \rightarrow Fe(III)$  and  $O_2^{2-} \rightarrow Fe(III)$  in model compounds to those of azidomet- and oxyhemerythrin respectively, (Table 2) suggest that peroxide in oxyhemerythrin and azide in azidomethemerythrin occupy the same site. Another aspect of hemerythrin chemistry revealed by the absorption spectra is the presence of an Fe(III) —  $O^{2-}$  — Fe(III)  $\mu$ -oxo-bridged unit in oxy- and methemerythrin (but not in deoxy-) [3,19] presumably arising from the reaction of Fe(III) with water [21]. The similarity in positions of near ultraviolet bands for several hemerythrin derivatives with those of known Fe(III)  $\mu$ -oxo-bridged compounds (Table 2) [3,19,22] suggests the presence of such a bridged unit in the protein.

#### (ii) Magnetic susceptibility

Further evidence for a  $\mu$ -oxo-bridge in hemerythrin arises from the ability



TABLE 2

Ligand-to-iron (III) charge-transfer energies in hemerythrin and model complexes [3]

Type	Hemerythrin complex		Type	Model complex	
	Ligand	Band energy (cm <sup>-1</sup> )		Ligand	Band energy (cm <sup>-1</sup> )
Oxyhemerythrin	O <sub>2</sub>	20,000		O <sub>2</sub> <sup>2-</sup> or O <sub>2</sub> H <sup>-</sup>	20,500
Methemerythrin	SCN <sup>-</sup>	22,200	(Fe <sup>III</sup> (H <sub>2</sub> O) <sub>5</sub> X) <sup>n+</sup>	SCN <sup>-</sup>	21,800— 22,400
	N <sub>3</sub> <sup>-</sup>	22,400		N <sub>3</sub> <sup>-</sup>	21,800— 22,200
	Br <sup>-</sup>	25,600		Br <sup>-</sup>	24,700
	Cl <sup>-</sup>	26,300		Cl <sup>-</sup>	29,400
	NCO <sup>-</sup>	26,500		NCO <sup>-</sup>	27,800— 28,500
	OH <sup>-</sup>	27,600		OH <sup>-</sup>	33,000
	O <sup>2-</sup>	30,000— 31,600		O <sup>2-</sup>	29,800
	H <sub>2</sub> O	40,000		H <sub>2</sub> O	41,700

of O<sup>2-</sup> to couple two iron atoms antiferromagnetically. This coupling is manifested by a decreased susceptibility to a magnetic field compared to isolated high spin Fe(III) and by a decreasing susceptibility with decreasing temperature. Oxy- and methemerythrins show both these properties and near absolute zero they become diamagnetic [23,24]. The exchange coupling constant,  $J$ , was found to be  $-77\text{ cm}^{-1}$  for oxyhemerythrin and  $-134\text{ cm}^{-1}$  for aquomethemerythrin [23], and can be compared to values of  $-90$  to  $-131\text{ cm}^{-1}$  for known  $\mu$ -oxo-bridged compounds [21]. Although other bridging ligands could conceivably produce antiferromagnetism, the magnitude of the coupling in hemerythrin strongly suggests that a  $\mu$ -oxo-bridge is responsible. The magnetic susceptibility of deoxyhemerythrin at room temperature is consistent with the four unpaired electrons per iron atom expected for high spin Fe(II) [25].

### (iii) Mössbauer spectra

Mössbauer spectra of several hemerythrin derivatives also suggest antiferromagnetism [25–27]. The pertinent parameters of isomer shift and quadrupole splitting listed in Table 3 classify the iron atoms as high spin Fe(II) in deoxyhemerythrin and as high spin Fe(III) in oxy- and several methemerythrins. The parameters for the latter derivatives closely resemble those of Fe(III)  $\mu$ -oxo-bridged compounds [2,4,21]. Furthermore, the spectra are unaffected by a 5 kgauss magnetic field at 4.2 K which indicates a diamagnetic ground state, i.e. antiferromagnetism [26,27]. Perhaps the most sig-

TABLE 3

Mössbauer properties of hemerythrin derivatives [26,27]

Complex	Ligand	Mössbauer Parameters	
		Isomer shift (mm sec <sup>-1</sup> )	Quadrupole splitting (mm sec <sup>-1</sup> )
Oxyhemerythrin	O <sub>2</sub>	0.46	1.87
		0.47	0.94
Methemerythrin	NCS <sup>-</sup>	0.55	-1.92
	Cl <sup>-</sup>	0.50	2.04
	F <sup>-</sup>	0.55	1.93
	N <sub>3</sub> <sup>-</sup>	0.50	1.91
	H <sub>2</sub> O	0.46	1.57
Deoxyhemerythrin	H <sub>2</sub> O	1.15	2.80

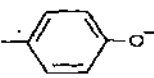
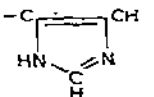
nificant result of the Mössbauer spectra is that oxyhemerythrin shows a pair of quadrupole split doublets, in contrast to deoxy- and methemerythrins, which show only a single doublet. Thus, Mössbauer spectra reveal two iron environments for oxyhemerythrin, but only one environment for deoxy- and methemerythrins.

(iv) *Chemical modification*

Since hemerythrin contains no porphyrin ring, the iron atoms must

TABLE 4

Possible protein ligands to the iron atoms in hemerythrin

Group	Amino acid residue	Number in hemerythrin	Conclusions from chemical modification	Ref.
-SH	Cys	1	not involved	8
-NH <sub>2</sub>	Lys	11	not involved	2, 29, 30
	NH <sub>2</sub> terminal	1	not involved	
	Tyr	5	Tyr-18, -70, not involved Tyr-8, -67, -109 are possible ligands	30, 31
	His	7	His-34, -73, or -77, and -82 are not involved His-25, -54, -73 or -77, and 101 are possible ligands	2, 29
-CO <sub>2</sub> <sup>-</sup>	Glu	6	not involved	28
	Asp	11	not involved	
	CO <sub>2</sub> terminal	1	not involved	
-S-CH <sub>3</sub>	Met	1	not involved	2, 29

be coordinated directly to amino acid residues. From examination of ligands in other iron-containing proteins and in model iron compounds [2] one can point to 44 of the 113 amino acid residues in hemerythrin as potential ligands to the irons and these are listed in Table 4. Those residues that chemical modification studies have ruled out, together with the remaining choices for ligands to the irons, are so indicated in Table 4. These results, together with comparisons of amino acid sequences from genetic variants [15,32], indicate that of the original 44 potential ligands, only 8 are actual possibilities: His-25, -54, -73 or -77, -101 and Tyr-8, -67 and -109 (sequence numbering follows Fig. 5).

*(v) X-ray crystallography*

Two independent X-ray diffraction studies of the iron site of hemerythrin have recently appeared, one of azidometmyohemerythrin [12], and one of aquomethemerythrin [33].

*(a) Azidometmyohemerythrin.* The structure of azidometmyohemerythrin has been solved at a resolution of 5.5 Å. The positions of the iron atoms, moreover, have been determined at a resolution of 2.8 Å and show an Fe --- Fe distance of  $3.44 \pm 0.05$  Å. Details of the structure between the iron atoms have not been resolved, but if the Fe—O distances are assumed to be 1.8 Å, a 3.44 Å Fe --- Fe distance gives an Fe—O—Fe  $\mu$ -oxo-bridging angle of  $145^\circ$ . This angle is within the range of model  $\mu$ -oxo-bridged compounds [21].

Each of the four long helical segments labeled A, B, C, and D and the fifth helical stub, designated E in Fig. 3, shows a connection of electron density to the iron site. A sixth connection projects from the CD corner. By alignment of the amino acid sequence of Fig. 5 with the electron density map of azidometmyohemerythrin, ligands to the iron atoms have been tentatively identified as His-25, His-54 and Tyr-109 for one Fe, His-73, His-101 and Tyr-67 for the other.

From the crystallographic data on azidometmyohemerythrin plus the spectroscopic, magnetic and chemical modification studies discussed above, the tentative picture of the active site that emerges is shown in Fig. 7 [2,12]. Dioxygen in the form of peroxide is bound to either one or both antiferromagnetically coupled high spin ferric irons which are separated by 3.44 Å and bridged by an  $O^{2-}$  ion. Two histidines and one tyrosine ligate each iron atom. Coordinating ligands, such as azide, may replace the peroxo group in oxyhemerythrin to form methemerythrin—ligand complexes.

*(b) Aquomethemerythrin.* An alternative model based on crystallographic results from *T. dyscritum* aquomethemerythrin at 2.8 Å resolution is shown in Fig. 8. In this structure His-77 replaces Tyr-67 of Fig. 7. However, the major difference is that in Fig. 8 two bridging ligands from the protein are presumed to occupy coordination positions 1 and 2 between the iron atoms.

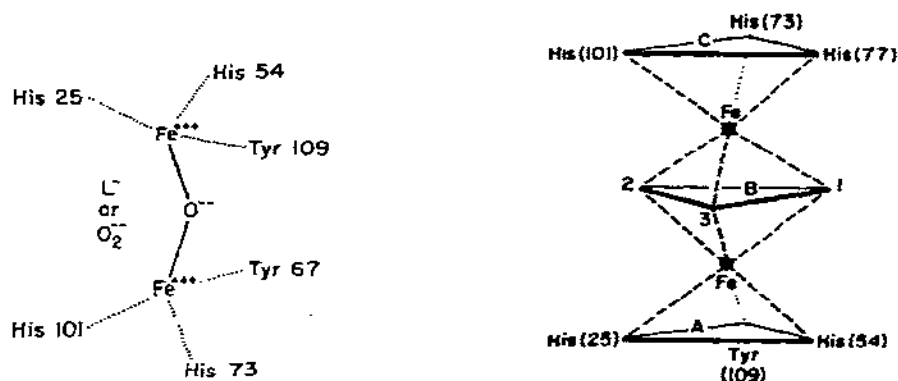


Fig. 7. Details of the probable structure at the oxygen binding site of hemerythrin. No specific coordination geometry is implied. Sequence numbering follows Fig. 5.

Fig. 8. Idealized representation of coordination positions about the iron atoms of *T. dyscritum* hemerythrin.

Alignment of the amino acid sequence of Fig. 5 with the electron density map shows that the bridging ligands are the carboxyl group of Asp-106 and the amide of Gln-58 (which would presumably bridge through the carbonyl oxygen). Coordination position 3 between the iron atoms (Fig. 8) is presumed to be occupied by water in aquomethemerythrin and by dioxygen in oxyhemerythrin. An accurate Fe - - Fe distance could not be determined from the electron density map, but the distance appears to be significantly less than the 3.44 Å determined for azidometmyohemerythrin, and may be less than 3 Å [34].

Thus, significant differences exist in the two models of the oxygen binding site deduced from X-ray diffraction studies. However, as discussed below the two crystallographic models are not necessarily incompatible since they are based on data from two different forms of hemerythrin, azidomet- and aquomet. Spectroscopic comparisons of hemerythrins from four different species of sipunculids reveal no differences in the active site [54].

#### (vi) Resonance Raman spectroscopy

IR and Raman spectroscopy are two methods that yield vibrational information about molecules. However, neither of these techniques is normally feasible for the examination of a single group of atoms embedded in a macromolecule. The intense absorption by water throughout the IR spectrum is also a serious drawback to the study of biological systems. Raman spectroscopy removes the problem of absorption by water, but the Raman spectrum of a colorless protein contains far too many low intensity peaks to allow a selective examination of vibrations at a specific site. Resonance enhancement of the intensity of a few vibrational modes in the Raman

spectrum of an absorbing protein removes the latter problem as well and thus makes resonance Raman spectroscopy a powerful probe of macromolecular structure.

Resonance enhancement may occur when an incident laser beam has a wavelength that falls underneath an allowed electronic absorption band of the scattering molecules. The resonance enhancement is most pronounced for those modes which resemble the molecular distortion that occurs upon the allowed electronic excitation. The resonance Raman spectra obtained with about 500 nm laser excitation for ligated hemerythrins agree with this generalization (Tsuboi's rule). Thus the most strongly resonance-enhanced features, inter-ligand and metal-ligand stretching modes, involve bands which should be significantly altered by the 500 nm ligand-to-metal charge-transfer transition [35].

(a) *Oxy- and azidomethemerythrin*. The charge transfer transitions of hemerythrin (Table 2 and Fig. 6) overlap several blue and green laser lines. For oxyhemerythrin the vibrations that are coupled to the  $O_2^{2-} \rightarrow Fe(III)$  charge transfer transition at 500 nm are localized at the oxygen binding site. Peaks at  $844\text{ cm}^{-1}$  and  $540\text{ cm}^{-1}$  in the resonance Raman spectrum of oxyhemerythrin (Fig. 9) have been assigned to symmetric O—O and Fe—O stretching frequencies, respectively, of dioxygen bound by hemerythrin [36,37]. These assignments were confirmed by showing the mass dependence of the peaks when  $^{18}O_2$  was substituted for  $^{16}O_2$ . The observed shift in the O—O stretching frequency, from  $844\text{ cm}^{-1}$  to  $798\text{ cm}^{-1}$ , agrees almost exactly

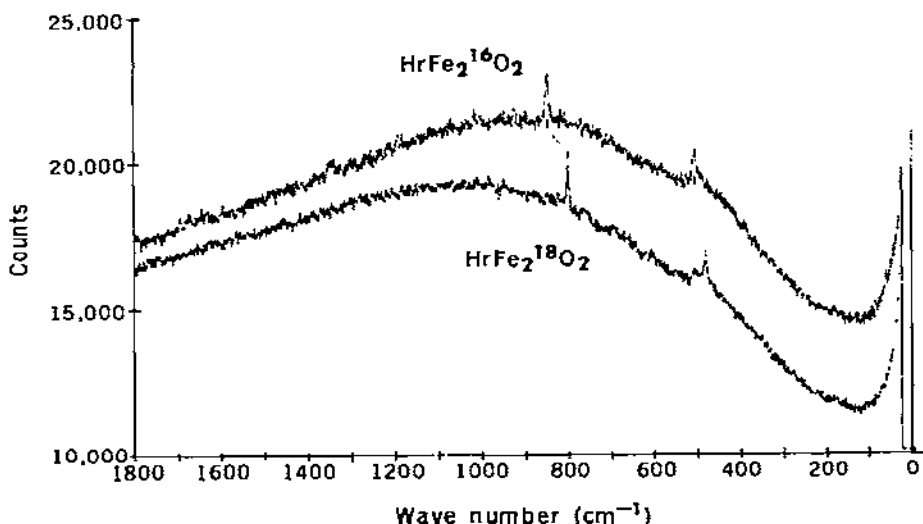


Fig. 9. Resonance Raman spectrum of oxyhemerythrin in solution, using 514.5 nm excitation.

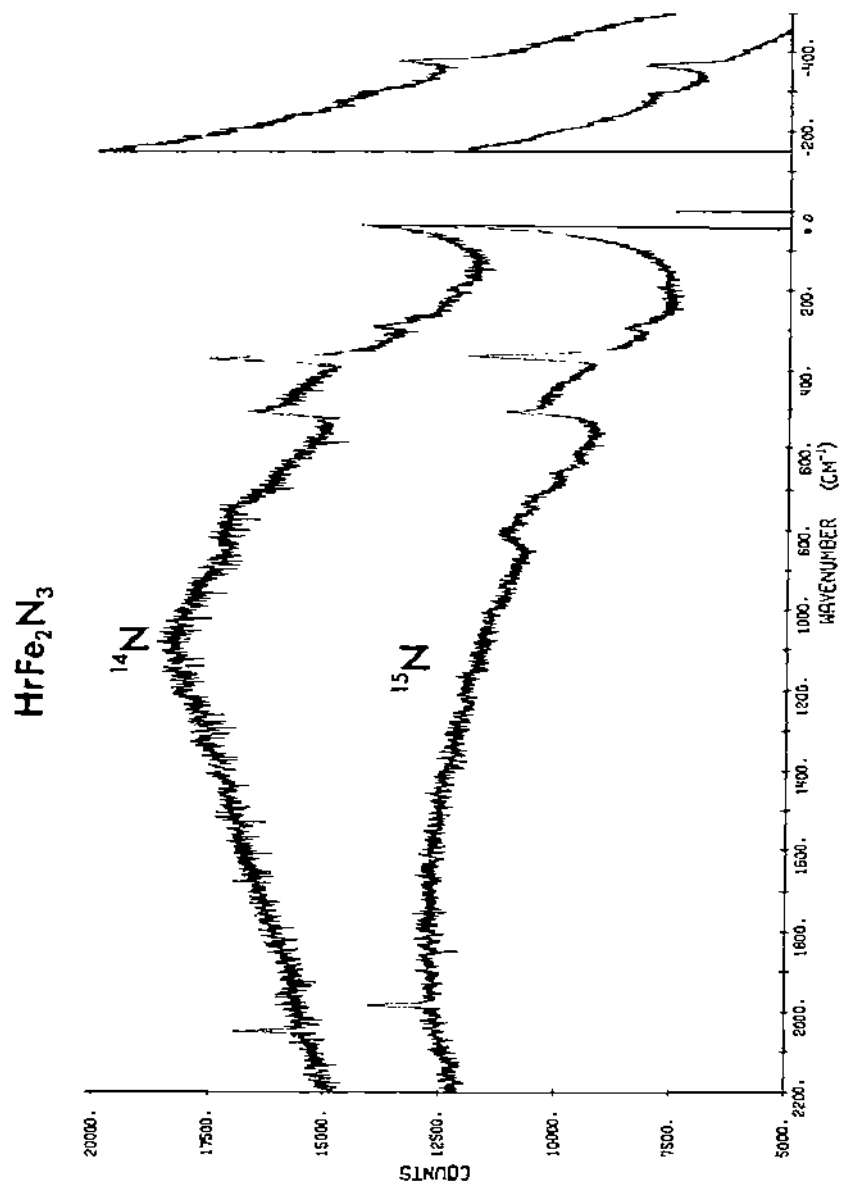


Fig. 10. Resonance Raman spectrum of azidomethemerythrin in solution using 514.5 nm excitation.

with the shift to  $796\text{ cm}^{-1}$  calculated for a diatomic oscillator. Comparison of O—O stretching frequencies with bond length and chemical information demonstrates that a useful correlation can be made between the frequencies and formal oxidation states of  $\text{O}_2$ ; thus the O—O stretch of molecular oxygen is  $1555\text{ cm}^{-1}$ , that for superoxide complexes is  $1100\text{--}1200\text{ cm}^{-1}$ , and for peroxide complexes it is  $740\text{--}900\text{ cm}^{-1}$  [37–39]. The O—O stretching frequency in oxyhemerythrin,  $844\text{ cm}^{-1}$ , clearly indicates a peroxide-type oxidation state for the bound dioxygen.

Azidomethemerythrin gives a resonance Raman spectrum [37] (Fig. 10) analogous to that of oxyhemerythrin, i.e. peaks are obtained at  $2050\text{ cm}^{-1}$  and  $376\text{ cm}^{-1}$  corresponding to asymmetric azide stretching and Fe—N stretching frequencies, respectively. A weak peak appears at  $292\text{ cm}^{-1}$  which is not sensitive to the mass of bound azide and which has been assigned to an Fe—N vibration of coordinated histidyl residues [37,54]. An additional peak is obtained in the resonance Raman spectrum of azidomethemerythrin at  $507\text{ cm}^{-1}$  which also is not sensitive to the mass of  $\text{N}_3^-$ . The peak is in the region of Fe—O vibrations and may be due either to tyrosine or carboxyl ligands to the irons or to a  $\mu$ -oxo-bridge vibration (see Section D. (vi) (d)). This same peak seems to appear weakly in resonance Raman spectra of oxyhemerythrin when  $^{18}\text{O}_2$  is used to shift  $\nu_{\text{FeO}}$  of bound dioxygen away from the  $500\text{ cm}^{-1}$  region. However, the peak is difficult to distinguish from that for the 10–20% of methemerythrin which is almost always present in preparations of oxyhemerythrin.

Thus, resonance Raman spectroscopy provides a direct confirmation of the early formulation for the formal oxidation state of dioxygen bound by hemerythrin. However, the preceding spectra provide little information about the mode of attachment of dioxygen or other ligands to the iron site. Therefore further resonance Raman studies have been carried out [40,41], which when combined with the previous spectroscopic, magnetic, and X-ray diffraction results, reveal a more detailed picture of the ligand binding site.

(b) *Thiocyanatomethemerythrin*. Thiocyanatomethemerythrin gives a resonance-enhanced Raman spectrum which is illustrated in Fig. 11. On the basis of vibrational frequencies for model compounds [42] the starred peaks at  $2043\text{ cm}^{-1}$  and  $840\text{ cm}^{-1}$  have been assigned to  $\nu_{\text{CN}}$  and  $\nu_{\text{CS}}$ , respectively, of the bound thiocyanate. This assignment was confirmed by examination of resonance Raman spectra of various isotopically labeled thiocyanates [40].  $\nu_{\text{CN}}$  shifts from  $2043\text{ cm}^{-1}$  to  $2017\text{ cm}^{-1}$  when  $^{15}\text{N}^{12}\text{C}^{32}\text{S}^-$  is substituted for  $^{14}\text{N}^{12}\text{C}^{32}\text{S}^-$  and  $\nu_{\text{CS}}$  shifts from  $840\text{ cm}^{-1}$  to about  $834\text{ cm}^{-1}$  when  $^{14}\text{N}^{12}\text{C}^{34}\text{S}^-$  is substituted for  $^{14}\text{N}^{12}\text{C}^{32}\text{S}^-$ . The feature at  $298\text{ cm}^{-1}$  in Fig. 11 probably contains an iron—thiocyanate frequency, even though no shift was detected when either  $^{15}\text{N}$  or  $^{34}\text{S}$  labeled thiocyanate was used. The peak at  $511\text{ cm}^{-1}$  in Fig. 11 corresponds to the  $507\text{ cm}^{-1}$  band in the spectrum of azidomethemerythrin.

Transition metal thiocyanates show a good correlation of vibrational fre-

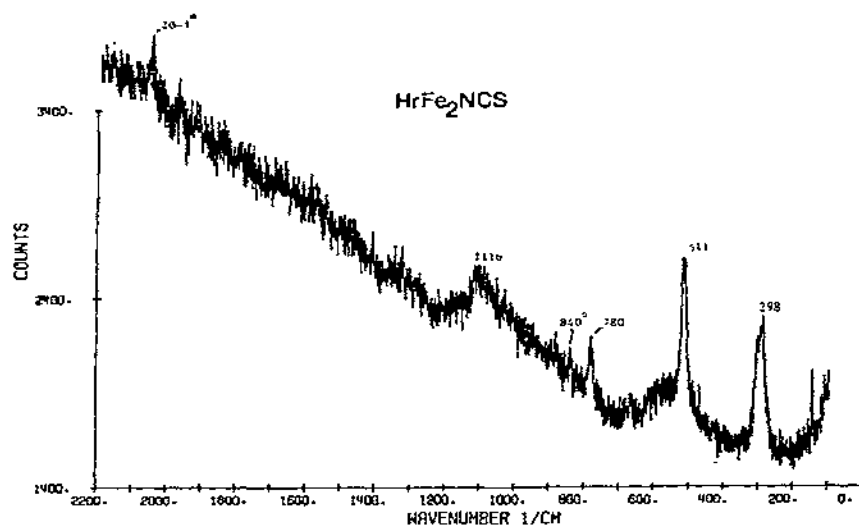
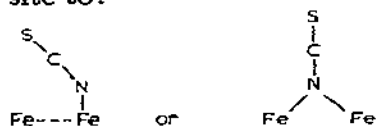


Fig. 11. Resonance Raman spectrum of thiocyanatomethemerythrin in solution using 457.9 nm excitation.

quencies with bonding geometry [42]. For  $\nu_{\text{CN}}$  the ranges are 2040–2080  $\text{cm}^{-1}$  for M–NCS and 2080–2120  $\text{cm}^{-1}$  for M–SCN. The range for M–SCN–M is broad and overlaps that for M–SCN but not that for M–NCS. For  $\nu_{\text{CS}}$  the ranges are distinct, 690–720  $\text{cm}^{-1}$  for S-bonded and 780–860  $\text{cm}^{-1}$  for N-bonded. On the basis of  $\nu_{\text{CN}}$  and  $\nu_{\text{CS}}$  criteria, thiocyanate can be classified as N-bonded in methemerythrin. This result reduces the number of choices for the mode of attachment of the single thiocyanate ion to the iron site to:



These two structures cannot be distinguished by vibrational frequencies because no compounds are known in which thiocyanate bridges two metal atoms through the nitrogen. This fact itself argues against a nitrogen bridged thiocyanate in methemerythrin. It might be thought, because of the known affinity of a dimeric iron center for bridging sulfur (e.g. the  $\text{Fe}_2\text{S}_2$  iron–sulfur proteins [43]), and because of the known ability of thiocyanate to bridge two metal atoms through its sulfur atom [44] that S-bridging would be more likely than N-bridging for thiocyanatomethemerythrin. Since the experimental data indicate N-bonding and since thiocyanate apparently prefers to bind to a single iron even in binuclear  $\mu$ -oxo-bridged compounds [45], the non-bridged structure would seem to be the more plausible choice. The possibility exists, nevertheless, that a unique environment provided by the protein stabilizes an N-bridged structure.



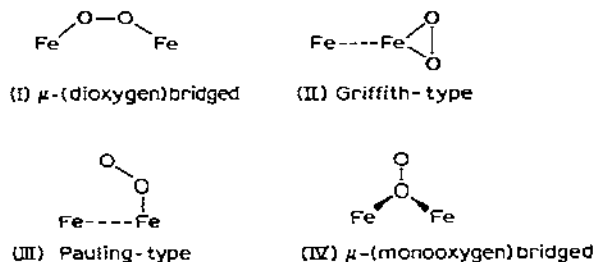
(c) *Other complexes of methemerythrin.* Resonance Raman spectra have been obtained of methemerythrin complexes of cyanamide and selenocyanate [68]. The spectrum of cyanamidomethemerythrin is analogous to that of azidomethemerythrin. Peaks are obtained at  $388\text{ cm}^{-1}$  and  $2169\text{ cm}^{-1}$  which are assigned to  $\nu_{\text{Fe}-\text{N}}$  and  $\nu_{\text{C}\equiv\text{N}}$ , respectively, of the bound cyanamide. Additional peaks are obtained at  $298\text{ cm}^{-1}$  and  $510\text{ cm}^{-1}$  which correspond to those obtained in the spectrum of azidomethemerythrin.

Selenocyanatomethemerythrin gives a spectrum analogous to that of thiocyanatomethemerythrin with  $\nu_{\text{CN}}$  at  $2043\text{ cm}^{-1}$ , and  $\nu_{\text{Fe}-\text{N}}$  at  $275\text{ cm}^{-1}$  ( $\nu_{\text{C}-\text{Se}}$  could not be identified above background). A strong peak is also obtained at  $515\text{ cm}^{-1}$ .

Thus, resonance Raman spectra of all methemerythrin-ligand complexes so far examined reveal metal-ligand and internal ligand vibrations plus a peak in the range of  $507\text{--}515\text{ cm}^{-1}$ .

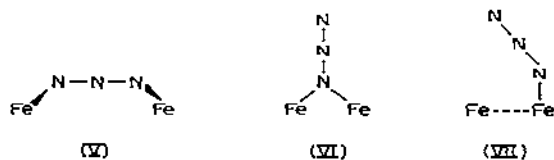
(d) *Unsymmetrically isotopic ligands.* A potentially powerful application of isotopes for vibrational analysis is provided by unsymmetrically isotopic ligands. The use of ligands such as  $^{16}\text{O}^{18}\text{O}$  and  $^{15}\text{N}^{14}\text{N}^{14}\text{N}^-$  can, in theory, discriminate among alternative geometric arrangements of ligands at a metal center.

For example, with dioxygen as ligand, several idealized structural representations have been suggested [3,4,18,19,23] for the functional center of hemerythrin



With  $^{16}\text{O}^{18}\text{O}$ , single symmetric O—O and Fe—O stretching frequencies,  $\nu_{\text{OO}}$  and  $\nu_{\text{FeO}}$ , respectively, would be expected for structures (I) and (II), whereas  $\nu_{\text{OO}}$  and  $\nu_{\text{FeO}}$  should each be doublets if dioxygen is bound as shown in (III) or (IV) because there are two possible modes of attachment of the unsymmetrical ligand.

Corresponding structures can be drawn with azide as ligand in place of dioxygen



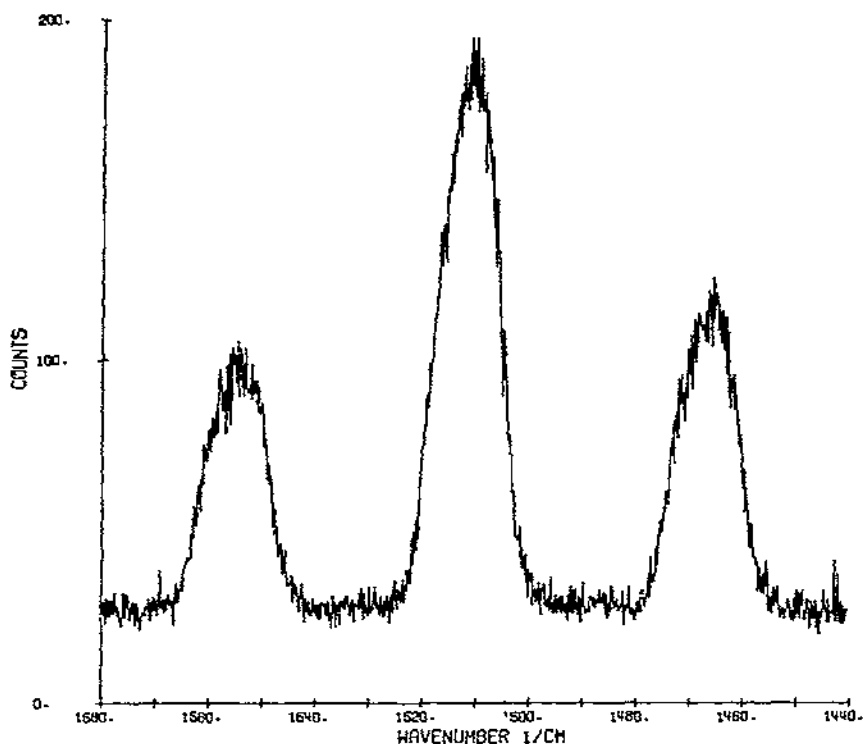


Fig. 12. Raman spectrum in the  $\nu_{\text{OO}}$  region of 58%  $^{18}\text{O}$  dioxygen gas using 457.9 nm excitation.

With  $^{15}\text{N}^{14}\text{N}^{14}\text{N}^-$ , splitting of the azide asymmetric stretch and the  $\Gamma\text{e}-\text{N}$  stretch,  $\nu_{\text{N}\equiv\text{N}}$  and  $\nu_{\text{Fe}-\text{N}}$ , respectively, would be expected for structures (VI) and (VII) but not for (V).

In view of the difficulty in obtaining a sample of pure  $^{16}\text{O}^{18}\text{O}$ , experiments on oxyhemerythrin were performed with a mixture of the isotopic species  $^{16}\text{O}_2$ ,  $^{16}\text{O}^{18}\text{O}$ , and  $^{18}\text{O}_2$ . A normal Raman spectrum of this gaseous dioxygen sample in the symmetric O—O stretching ( $\nu_{\text{OO}}$ ) region (Fig. 12) reveals relative peak areas of 1 : 2.1 : 1.2 for  $\nu_{\text{OO}}$  of  $^{16}\text{O}_2$ ,  $^{16}\text{O}^{18}\text{O}$ , and  $^{18}\text{O}_2$ , respectively. The resonance Raman spectrum of oxyhemerythrin prepared with this same dioxygen sample (Fig. 13) shows three bands in the O—O stretching region with relative areas 1 : 2.3 : 1.3 but with the central peak much reduced in height compared to that in Fig. 12. Furthermore, the central peak of Fig. 13, which represents  $\nu_{\text{OO}}$  for  $^{16}\text{O}^{18}\text{O}$ , is significantly broader ( $10.0\text{ cm}^{-1}$  at half-height) than the  $^{16}\text{O}_2$  ( $7.1\text{ cm}^{-1}$ ) and  $^{18}\text{O}_2$  ( $5.4\text{ cm}^{-1}$ ) peaks, and the top of the peak is flattened. Spectra obtained at slightly higher resolution [41] show a central depression of the  $^{16}\text{O}^{18}\text{O}$  peak. All these observations indicate that two closely spaced features contribute to the

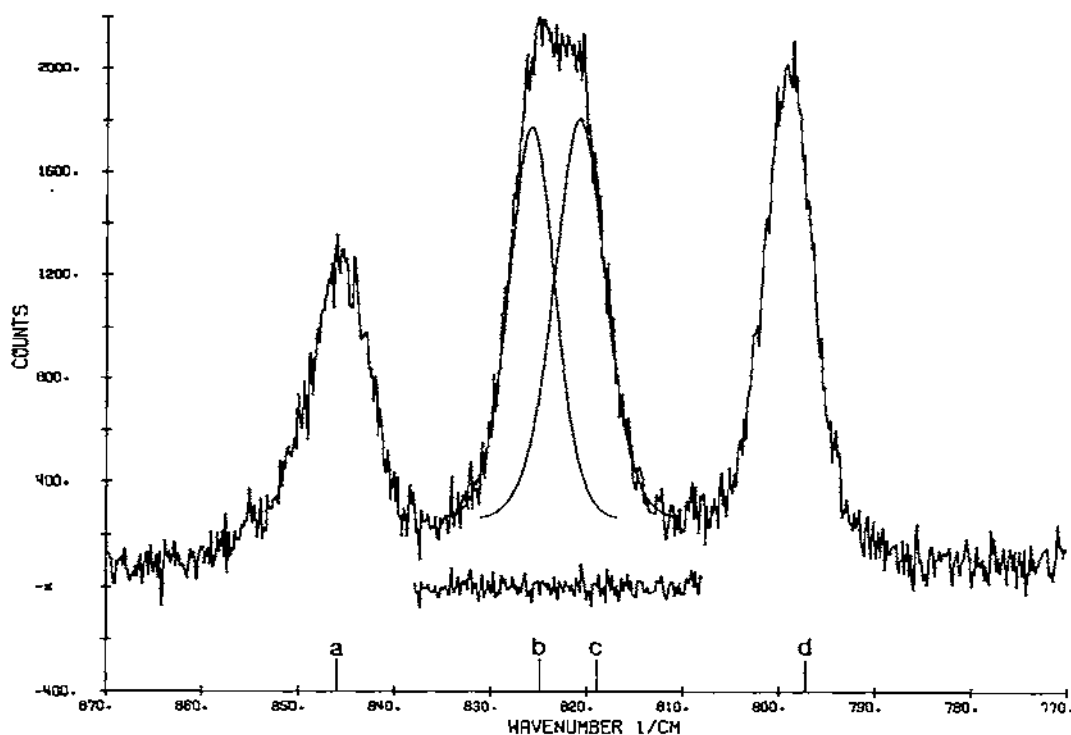


Fig. 13. Resonance Raman spectrum in the  $\nu_{\text{OO}}$  region of oxyhemerythrin (3 mM in monomer) prepared with the dioxygen gas of Fig. 12. The smooth curves represent deconvolution of the  $822\text{ cm}^{-1}$  feature into two components. The difference between observed and fitted curves is shown below the spectrum near  $822\text{ cm}^{-1}$ . The vertical lines a, b, c and d show the calculated peak positions for models (III) and (IV) of  $\text{Fe-}^{16}\text{O}_2$  ( $846\text{ cm}^{-1}$ ),  $\text{Fe-}^{16}\text{O-}^{18}\text{O}$  ( $825\text{ cm}^{-1}$ ),  $\text{Fe-}^{18}\text{O-}^{16}\text{O}$  ( $819\text{ cm}^{-1}$ ) and  $\text{Fe-}^{18}\text{O}_2$  ( $798\text{ cm}^{-1}$ ), respectively.

$822\text{ cm}^{-1}$  band. In fact, a good least squares fit of this band may be achieved by the use of two components of  $5.5\text{ cm}^{-1}$  width, at half-height, separated by  $5\text{ cm}^{-1}$  (Fig. 13). The difference between the observed spectrum and the composite of the fitted curves (Fig. 13) is flat and at about the noise level of the observed spectrum, which indicates an accurate fit. Also, a single peak (Lorentzian—Gaussian function) does not give a good least squares fit to the experimental data, again indicating the composite nature of the central feature in Fig. 13.

The Fe—O stretching ( $\nu_{\text{FeO}}$ ) region in the vicinity of  $490\text{ cm}^{-1}$  (Fig. 14) [41] of a sample of oxyhemerythrin whose  $\nu_{\text{OO}}$  region indicated a 1 : 2.4 : 1.4 ratio of  $^{16}\text{O}_2$  :  $^{16}\text{O}^{18}\text{O}$  :  $^{18}\text{O}_2$  shows only two peaks at positions very close to those for  $\nu_{\text{FeO}}$  of  $\text{HrFe}_2^{16}\text{O}_2$  and  $\text{HrFe}_2^{18}\text{O}_2$ . The central  $^{16}\text{O}^{18}\text{O}$  peak is apparently missing.

Calculated frequencies provide a ready interpretation of both regions of

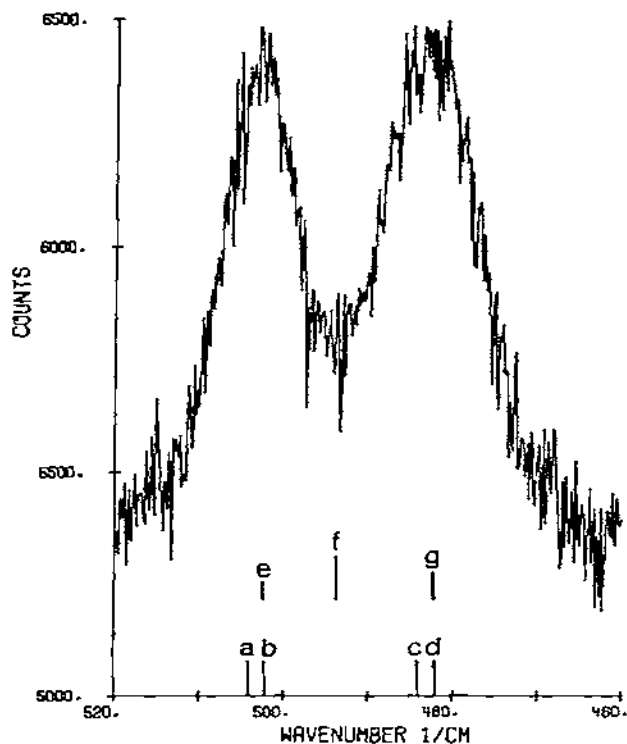


Fig. 14. Resonance Raman spectrum in the  $\nu_{\text{FeO}}$  region of oxyhemerythrin (4 mM in monomer) prepared with 58%  $^{18}\text{O}$  dioxygen gas. Vertical lines *a*, *b*, *c* and *d* show the calculated peak positions for models (III) and (IV) of  $\text{Fe}-^{16}\text{O}_2$  ( $504\text{ cm}^{-1}$ ),  $\text{Fe}-^{16}\text{O}-^{18}\text{O}$  ( $502\text{ cm}^{-1}$ ),  $\text{Fe}-^{16}\text{O}-^{16}\text{O}$  ( $484\text{ cm}^{-1}$ ),  $\text{Fe}-^{18}\text{O}_2$  ( $482\text{ cm}^{-1}$ ), respectively. Vertical lines *e*, *f*, and *g* show for models (I) and (II) the calculated peak positions and estimated relative intensities of the  $^{16}\text{O}_2$  ( $502\text{ cm}^{-1}$ , 1),  $^{16}\text{O}^{18}\text{O}$  ( $494\text{ cm}^{-1}$ , 2.4) and  $^{18}\text{O}_2$  ( $482\text{ cm}^{-1}$ , 1.4) complexes, respectively.

the resonance Raman spectrum of oxyhemerythrin in the presence of  $^{16}\text{O}^{18}\text{O}$ . Values of the simple valence force constants,  $f_{\text{OO}}$  and  $f_{\text{FeO}}$ , were calculated [40,46–48] for each of the structural models (I)–(IV) from the observed frequencies of  $\text{HrFe}_2^{16}\text{O}_2$  and  $\text{HrFe}^{18}\text{O}_2$ . Where it was needed, an  $\text{Fe}-\text{O}-\text{O}$  bending force constant was estimated as  $(0.1-0.5)f_{\text{FeO}}$ . These force constants were then used to calculate frequencies for each of the  $^{16}\text{O}^{18}\text{O}$  structural models. In Fig. 13, vertical lines *a*, *b*, *c*, and *d* show the calculated frequencies in the  $\text{O}-\text{O}$  stretching region for models (III) and (IV), which are in quite good agreement with the observed spectrum. The calculated frequencies for models (I) and (II), on the other hand, predict only a single band at  $822\text{ cm}^{-1}$  for  $^{16}\text{O}^{18}\text{O}$ . The  $\text{Fe}-\text{O}$  stretching region can also be readily explained in terms of structural models such as (III) and (IV). The vibrational analyses for these two models demonstrate that  $\nu_{\text{FeO}}$  for  $\text{Fe}-^{16}\text{O}-^{18}\text{O}$  should nearly overlap that for  $\text{Fe}-^{16}\text{O}-^{16}\text{O}$ , and a similar near

coincidence is calculated for  $\text{Fe}-^{18}\text{O}-^{16}\text{O}$  with  $\text{Fe}-^{18}\text{O}-^{18}\text{O}$ . The calculated peak positions for models (III) and (IV) are indicated by vertical lines *a*, *b*, *c*, and *d* in Fig. 14. Once again, models (I) and (II) predict a single  $^{16}\text{O}^{18}\text{O}$  peak between those for  $^{16}\text{O}_2$  and  $^{18}\text{O}_2$ , and their positions and estimated relative intensities are indicated by vertical lines *e*, *f*, and *g* in Fig. 14. Additional calculations indicate that the observed data are consistent with the inclusion of a  $\mu$ -oxo-bridge in models (III) and (IV).

The effect of distortion of the Griffith-type structure and of the  $\mu$ -(dioxygen)-bridged model on the isotopic splittings was also evaluated. Although distorted structures such as



are possible, it is estimated that a substantial difference (of the order of 1 mdyn  $\text{\AA}^{-1}$ ) in the two  $f_{\text{FeO}}$  values for each distorted structure is necessary to reproduce the observed  $^{16}\text{O}^{18}\text{O}$  splittings. For example an attempt was made to fit all the isotopic data using the  $\mu$ -(dioxygen)-bridged structural model. This refinement led to widely different values (1.8 and 0.2 mdyn  $\text{\AA}^{-1}$ ) for the two Fe—O stretching force constants, indicating that if the  $\mu$ -(dioxygen)-bridged structure does exist for oxyhemerythrin, the Fe—O—O—Fe bridge is highly asymmetric. Therefore, it is unlikely that the different environments for the two ends of oxygen arise from different ligand environments for the two iron atoms, with an otherwise nearly symmetric Fe—O—O—Fe bridge.

A corresponding experiment was performed with another unsymmetrically isotopic ligand,  $^{15}\text{N}^{14}\text{N}^{14}\text{N}^-$ , in place of  $^{16}\text{O}^{18}\text{O}$ . Examination of the resonance Raman spectrum of azidomethemerythrin prepared with  $\text{K}^{15}\text{N}^{14}\text{N}^{14}\text{N}$  of 99% isotopic purity reveals two clearly resolved peaks in the azide asymmetric stretching  $\nu_{\text{N}\equiv\text{N}}$  region, Fig. 15. These peaks at 2044  $\text{cm}^{-1}$  and 2032  $\text{cm}^{-1}$  are both clearly distinct from those of  $\text{HrFe}^{14}\text{N}_3$  (2050  $\text{cm}^{-1}$ ) and  $\text{HrFe}_2^{15}\text{N}_3$  (1983  $\text{cm}^{-1}$ ). This spectrum is incompatible with a structure such as (V), but is consistent with either (VI) or (VII) which are analogues of (III) and (IV).

Although quantitation is difficult, the observed 12  $\text{cm}^{-1}$  splitting of  $\nu_{\text{N}\equiv\text{N}}$  in spectra of  $\text{HrFe}_2^{15}\text{N}^{14}\text{N}^{14}\text{N}$  is probably too large to be ascribed to hydrogen bonding to, or protonation of, one of the nitrogen atoms in structure (V). Furthermore, although kinetic data on ligand exchange indicate that the azide binding site is accessible to water [49], no shifts in  $\nu_{\text{N}\equiv\text{N}}$  or  $\nu_{\text{Fe}-\text{N}}$  are observed in  $\text{D}_2\text{O}$ . Although small changes in  $\nu_{\text{OO}}$  and  $\nu_{\text{FeO}}$  are noted for oxyhemerythrin in  $\text{D}_2\text{O}$  [40] the putative splitting of  $\nu_{\text{FeO}}$  of 17–20  $\text{cm}^{-1}$  for  $\text{HrFe}_2^{16}\text{O}^{18}\text{O}$  is probably too large to be ascribed to protonation of one of the oxygen atoms of models (I) or (II) unless there is concomitant distortion of the Fe—O bonds.

Thus, resonance Raman spectra of hemerythrin in the presence of unsymmetrically isotopic ligands indicate that the correct structures contain indi-

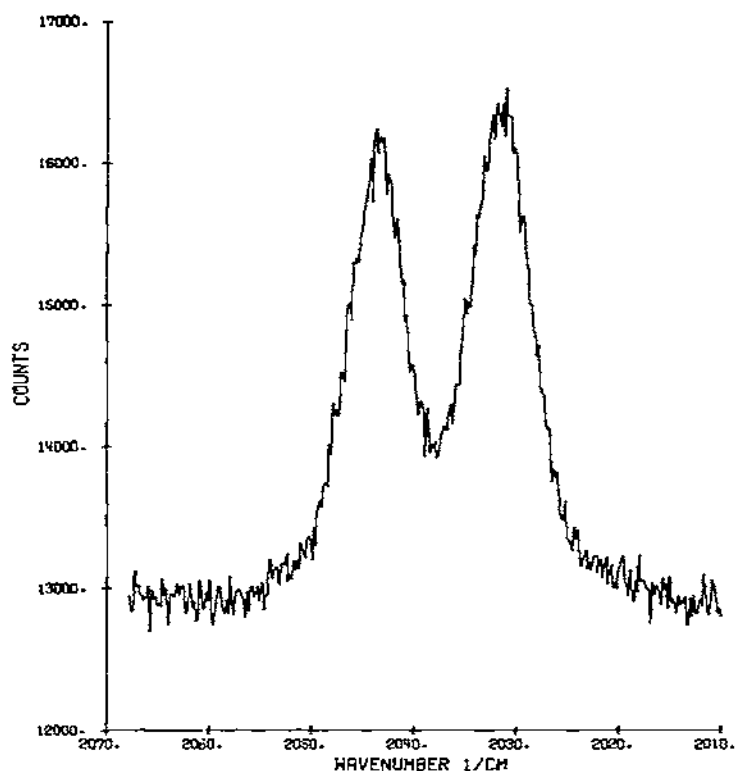
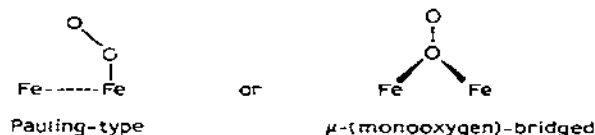


Fig. 15. Resonance Raman spectrum in the  $\nu_{N\equiv N}$  region of azidomethemerythrin prepared with  $K^{15}N^{14}N^{14}N$ .

vidual O and N atoms of  $O_2$  and  $N_3^-$ , respectively, in non-equivalent positions. The non-equivalent Mössbauer environments for the iron atoms of oxyhemerythrin suggest that a  $\mu$ -(dioxygen)-bridged structure such as (I) could produce vibrationally non-equivalent environments of the individual O atoms of bound dioxygen. As discussed above, however, such non-equivalence could be produced only by a difference in the strengths of the two Fe—O bonds. Similarly, the Griffith-type structure (II) might be acceptable if the Fe which coordinates  $O_2$  itself has an asymmetric ligand environment (as suggested by a referee). Once again, however, vibrational non-equivalence implies a difference in the two  $f_{FeO}$  values. Each of these distorted structures approaches an idealized Pauling-type structure such as (III) for a large difference in the two  $f_{FeO}$  values. An important point is that, despite equivalent Mössbauer environments for the iron atoms of azidomethemerythrin, the terminal N atoms of bound azide are vibrationally non-equivalent, just as are the O atoms of bound dioxygen.  $O_2$  and  $N_3^-$  may, therefore, be bound in analogous geometric dispositions. Although we do not rule out distorted  $\mu$ -(dioxygen)-bridged or Griffith-type structures, the data suggest

that, of the previously proposed idealized models (I)—(IV) for attachment of dioxygen to the iron site, only two possibilities remain



(e) *Oxygen-18 Water*. Resonance Raman spectra of hemerythrin derivatives have been examined in oxygen-18 water with the aim of detecting vibrational modes of a  $\mu$ -oxo-bridge, whose oxygen atom presumably should be exchangeable with water [21]. A resonance Raman spectrum, with the 514.5 nm exciting line, of oxyhemerythrin dissolved in 96.6%  $^{18}\text{O}$  water produced the usual  $844\text{ cm}^{-1}$  and  $504\text{ cm}^{-1}$  bands after a cycle of deoxygenation and reoxygenation (a deoxy-reoxy cycle) during which the  $\mu$ -oxo-bridge is presumably broken and reformed. No shifts in peak position could be detected. However, when the same solution was converted to azidomethemerythrin by azide displacement of peroxide, the spectrum in Fig. 16 was obtained. In

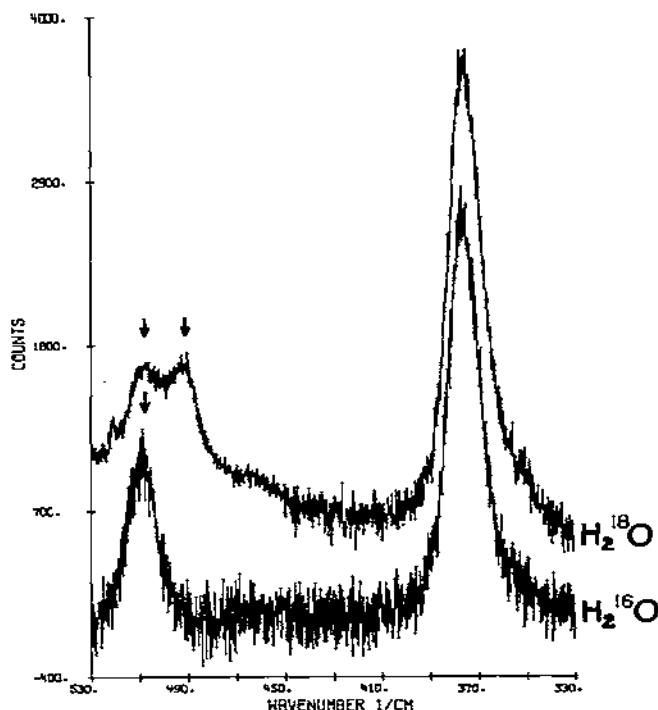


Fig. 16. Resonance Raman spectra of azidomethemerythrin in  $\text{H}_2^{16}\text{O}$  and  $\text{H}_2^{18}\text{O}$ . The hemerythrin in  $\text{H}_2^{18}\text{O}$  underwent one deoxy-reoxy cycle before conversion to azidomethemerythrin.

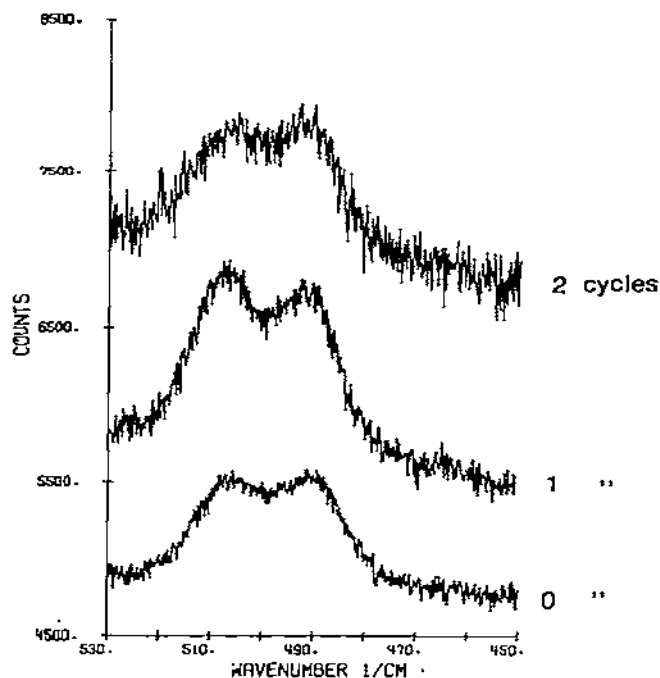


Fig. 17. Resonance Raman spectra of azidomethemerythrin solutions in  $\text{H}_2^{18}\text{O}$  that have undergone 0, 1 and 2 deoxy-reoxy cycles.

$\text{H}_2^{18}\text{O}$ ,  $\nu_{\text{Fe-N}}$  is at its normal position at  $376\text{ cm}^{-1}$ , but the peak at  $507\text{ cm}^{-1}$  in  $\text{H}_2^{16}\text{O}$  is split in  $\text{H}_2^{18}\text{O}$ . Approximately half the intensity has shifted to  $491\text{ cm}^{-1}$ . No other peaks in the spectrum show any shift or splitting. The approximate 50 : 50 ratio of peak intensities at  $507\text{ cm}^{-1}$  and  $491\text{ cm}^{-1}$  may be caused by partial exchange of the  $\mu$ -oxo-bridging oxygen, but if so, it is not due to the one deoxy-reoxy cycle undergone by the oxyhemerythrin before conversion to azidomethemerythrin. Figure 17 contains scans of solutions of azidomethemerythrin in  $\text{H}_2^{18}\text{O}$  that have undergone 0, 1, and 2 deoxy-reoxy cycles, respectively, before conversion to the azidomet form. No significant differences in peak ratios are evident.

Mass spectral analyses of these solutions gave 80–83%  $^{18}\text{O}$  water [40], which shows that the 50 : 50 peak ratio is not due to dilution of the water to 50%  $^{18}\text{O}$  upon introduction of the protein.

The peak remaining at  $507\text{ cm}^{-1}$  in  $\text{H}_2^{18}\text{O}$  is also not due to an  $^{16}\text{O}$  atom of dioxygen which was somehow incorporated during the conversion from oxy- to azidomethemerythrin. To discount this possibility, spectra were obtained [40] of an identical preparation of azidomethemerythrin in which the isotopes were reversed, i.e. using  $\text{H}_2^{16}\text{O}$  and  $^{18}\text{O}_2$ . No peak shifts or splittings could be detected. Clearly  $^{18}\text{O}$  was not incorporated from  $^{18}\text{O}_2$ .

No shift of the  $507\text{ cm}^{-1}$  band was observed in  $\text{D}_2\text{O}$ , indicating that this



band is not due to  $\nu_{\text{FeO}}$  of coordinated water or hydroxide.

Thus, the shift in peak position from  $507\text{ cm}^{-1}$  to  $491\text{ cm}^{-1}$  in spectra of azidomethemerythrin in  $\text{H}_2^{18}\text{O}$  seems to confirm the presumption of a  $\mu$ -oxo-bridge, but the splitting, instead of a complete (i.e. 80–83%) shift in intensity, is puzzling. The simplest interpretation is that the  $507\text{ cm}^{-1}$  band is a composite of two peaks, one of which is due to an iron–tyrosine vibration and the other to an Fe–O–Fe vibration. Several lines of evidence suggest that one or more tyrosines are ligands to the iron atoms in hemerythrin [12,30,31,33]. Moreover, phenolic oxygens normally do not exchange with those of water [50]. Resonance Raman spectra of the iron transport protein, transferrin, show that the C–O stretching frequency of the tyrosine ligands to iron(III) is unaffected by water which is 70%  $^{18}\text{O}$  [51]. Thus, the remaining intensity at  $507\text{ cm}^{-1}$  could be due to  $\nu_{\text{FeO}}$  of the non-exchangeable oxygen of coordinated tyrosine, while the intensity at  $491\text{ cm}^{-1}$  could be due to  $\nu_{\text{Fe-O-Fe}}$  of the  $\mu$ -oxo-bridge, whose oxygen is exchangeable with water.

The  $507\text{ cm}^{-1}$  frequency is in the correct range for the symmetric stretch of a bent  $\mu$ -oxo-bridge [52,53]. A normal coordinate analysis [52] of the  $C_{2v}$  system



shows that the percentage change in frequency on substitution of  $^{18}\text{O}$  for  $^{16}\text{O}$  is a function of the bridging angle  $\phi$ . From the secular equation for the symmetric  $[A_1]$  vibration, the  $507\text{ cm}^{-1}$  to  $491\text{ cm}^{-1}$  shift observed in azidomethemerythrin gives a calculated value of  $130^\circ$  for  $\phi$ . If the Fe–O distances are taken to be  $1.90\text{ \AA}$ , the  $130^\circ$  bridging angle gives an Fe–Fe distance of  $3.45\text{ \AA}$ , which is identical to that determined in azidometmyohemerythrin [12]. (The normal Fe–O distances for a  $\mu$ -oxo-bridge of  $1.8\text{ \AA}$  [21] give a reasonable Fe–Fe distance of  $3.25\text{ \AA}$ .)

The possibility exists that the observed behavior in  $\text{H}_2^{18}\text{O}$  is due to exchange of  $^{18}\text{O}$  with a carboxyl ligand to the irons. The X-ray structure of the iron site of aquomethemerythrin described by Stenkamp et al. [33] suggests that a carboxyl group from aspartic acid and a carbonyl group from glutamine bridge the two iron atoms. However, all 18 carboxyl groups of chloromethemerythrin can be amidated with glycine methyl ester without destruction of the active site as judged by absorption spectra [28]. This result suggests that aspartate is not a ligand.

Resonance Raman spectra of chloromethemerythrin contain a band at  $511\text{ cm}^{-1}$  corresponding to the  $507\text{ cm}^{-1}$  band in azidomethemerythrin [54]. Its behavior in the glycine-amidated protein or in  $\text{H}_2^{18}\text{O}$  has not yet been investigated.

The absence of splitting or a shift in the peak near  $500\text{ cm}^{-1}$  in spectra of oxyhemerythrin in  $\text{H}_2^{18}\text{O}$  is not surprising since, as discussed previously, the predominant intensity in this region is due to  $\nu_{\text{Fe-O}}$  of the bound dioxygen.

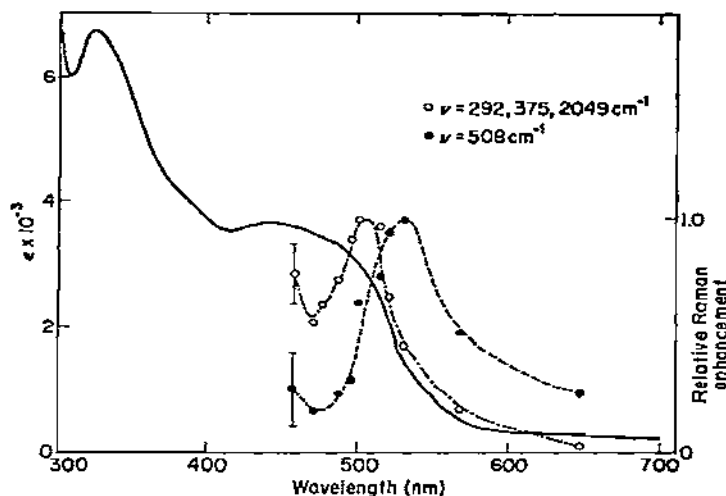


Fig. 18. Excitation profiles of the resonance Raman bands of azidomethemerythrin. Taken from [54] with permission of authors.

The reduction or absence of intensity of the  $507\text{ cm}^{-1}$  band in spectra of oxyhemerythrin compared to those of azidomethemerythrin could be due either to a ligand change, i.e. the absence of a  $\mu$ -oxo-bridge, or to a conformational change at the iron site which either reduces vibronic coupling or shifts the energy of the electronic transition to which the vibrational mode is coupled.

It is possible to prove that a vibrational peak in the resonance Raman spectrum is coupled to a specific electronic transition by measurement of an excitation profile. A spectrum of the intensity of the resonance enhanced peak is obtained relative to that of an internal standard as the incident laser frequency is varied over the electronic absorption band of the scatterer. Excitation profiles of the resonance Raman bands of azidomethemerythrin [54] (Fig. 18) show that the  $507\text{ cm}^{-1}$  band is coupled to an electronic transition at about  $530\text{ nm}$ , while the other three bands are coupled to a transition at about  $505\text{ nm}$ . This result demonstrates that the chromophore responsible for the  $507\text{ cm}^{-1}$  band is distinct from that responsible for the other ligand bands. The possibility that the  $507\text{ cm}^{-1}$  and  $491\text{ cm}^{-1}$  bands observed in  $\text{H}_2^{18}\text{O}$  have different excitation profiles has not yet been tested.

Thus, the behavior of the  $507\text{ cm}^{-1}$  band of azidomethemerythrin in  $\text{H}_2^{18}\text{O}$  can be regarded as tentative confirmation of a  $\mu$ -oxo-bridge, but the possibility of an iron-carboxylate vibration cannot be ruled out without further experimentation. An insight into the structure of the iron site of oxyhemerythrin using  $\text{H}_2^{18}\text{O}$  can only be inferred from the results on azidomethemerythrin.

(vii) *Models for the oxygen binding site of hemerythrin*

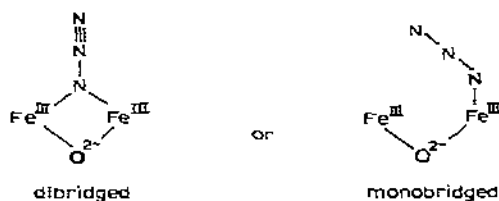
The results of the resonance Raman investigations require that any model for the ligand binding sites and for the interconversion between the various states of hemerythrin satisfy certain specifications:

1. Thiocyanate is probably N-bonded and, therefore, it is bound to only one iron.
2. Substitution of H<sub>2</sub>O by D<sub>2</sub>O produces a small perturbation of  $\nu_{\text{OO}}$  and  $\nu_{\text{FeO}}$  of oxyhemerythrin but no effect on  $\nu_{\text{N}\equiv\text{N}}$  and  $\nu_{\text{FeN}}$  of azidomethemerythrin.
3. The environments of O and N atoms in oxy- and azidomethemerythrin, respectively, are non-equivalent.
4. The oxygen atom of an Fe—O bond in azidomethemerythrin is exchangeable with water.

Results of other studies supply additional requirements:

5. Non-equivalent Mössbauer environments for the iron atoms in oxyhemerythrin, but equivalent environments for those in deoxy- and methemerythrins.
6. Antiferromagnetic coupling between the two iron atoms in oxy- and methemerythrins.
7. Similarity in absorption spectra of oxy- and several methemerythrins (but not aquomet).
8. Lack of proton uptake or release upon oxygenation of deoxyhemerythrin [4].
9. The peroxide-type electronic state of dioxygen bound by hemerythrin.
10. The 3.44 Å Fe—Fe distance in azidometmyohemerythrin, and the apparent discrepancy between X-ray structures of azidomet- and aquomethemerythrin.

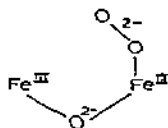
For azidomethemerythrin, the 3.44 Å Fe—Fe distance, the nonequivalent environments of the N atoms and a  $\mu$ -oxo-bridge to account for the antiferromagnetism lead to two choices for the azide binding site



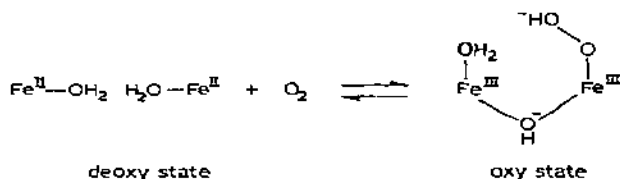
For the dibridged structure, at a 3.44 Å Fe—Fe separation the N—Fe—O angles would be about 50° for any reasonable Fe—N and Fe—O distances. This angle is too acute for adjacent coordination positions. Furthermore, the nonbonded N - - O distance would be much less than the sum of van der Waals' radii of N and O atoms. Therefore, the monobridged structure is more likely for azidomethemerythrin. This conclusion is also consistent with the resonance Raman results on thiocyanatomethemerythrin. Ligation of the

iron atoms by tyrosines can then explain the peak splitting observed in  $\text{H}_2^{18}\text{O}$ .

If oxyhemerythrin has a structure similar to that of azidomethemerythrin, as indicated by their absorption spectra and by nonequivalent environments of the O atoms, then a monobridged structure is also likely, with dioxygen bound as peroxide in a Pauling-type geometry

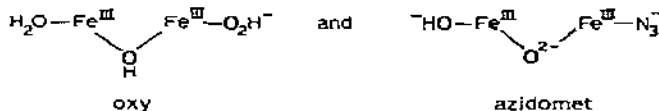


If one assumes further that the oxo oxygen and peroxide dioxygen can both be protonated, then the lack of proton uptake or release upon oxygenation of deoxyhemerythrin can be interpreted in terms of the equation



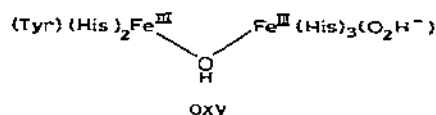
This proposed oxy-structure also accounts for the effect of  $\text{D}_2\text{O}$  on  $\nu_{\text{OO}}$  and  $\nu_{\text{FeO}}$ , just as the proposed azidomet- structure explains the lack of effect of  $\text{D}_2\text{O}$  on  $\nu_{\text{N}\equiv\text{N}}$  and  $\nu_{\text{FeN}}$ . Protonation of the  $\mu$ -oxo-bridge is likely to decrease the  $\text{Fe}-\text{O}-\text{Fe}$  angle [55,56]. The absence in resonance Raman spectra of oxyhemerythrin of an  $\text{Fe}-\text{O}$  peak that is sensitive to  $\text{H}_2^{18}\text{O}$  could be due to the change in angle from that in azidomethemerythrin. This change may alter the electronic transition, and, thereby decrease the resonance enhancement. The  $\mu$ -hydroxo-bridged structure is a proposed intermediate in the mechanism of  $\mu$ -oxo-dimer formation by  $\text{Fe}^{\text{III}}(\text{EDTA})^-$  [56]. The proposed binding of dioxygen in the form of a hydroperoxide to one iron has a precedent in the mononuclear  $\text{Fe}^{\text{III}}(\text{EDTA})^-$  complex of peroxide or hydroperoxide [57], which has an absorption maximum near 500 nm, the value observed in oxyhemerythrin.

The non-equivalent environments of the iron atoms in oxyhemerythrin and the equivalent environments in methemerythrin, as determined by Mössbauer spectroscopy can be rationalized [4] by structures such as

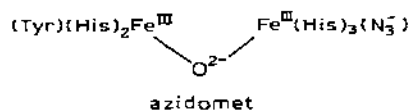


It is possible that  $\text{OOH}^-$  (or  $\text{O}_2^{2-}$ ) has a different effect on iron(III) than does  $\text{H}_2\text{O}$ , but that  $\text{N}_3^-$ ,  $\text{SCN}^-$ ,  $\text{Cl}^-$  etc. have effects on iron(III) similar to that of  $\text{OH}^-$ . Alternatively, different ligands from the protein to the two iron atoms,

as proposed by Stenkamp et al. [33], may produce the observed effect [58]:

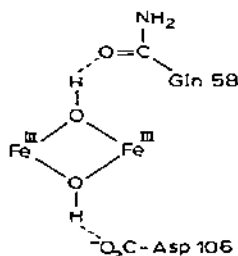


and



In these structures one assumes that Tyr—O<sup>−</sup> and N<sub>3</sub><sup>−</sup> have comparable effects on the two iron environments, but that Tyr—O<sup>−</sup> and O<sub>2</sub>H<sup>−</sup> (or O<sub>2</sub><sup>2−</sup>) do not.

Aquomethemerythrin (methemerythrin at pH 7) may have the following structure:



This structure has been suggested previously [58] as an alternative to that proposed for aquomethemerythrin by Stenkamp et al. [33]. The  $\mu$ -dihydroxo-bridged structure has precedents in iron(III) chemistry [55], and is a proposed intermediate in the formation of  $\mu$ -oxo-bridged compounds [21]. Although the observed antiferromagnetic coupling constant for aquomethemerythrin [23],  $J = -134 \text{ cm}^{-1}$ , is high for a  $\mu$ -dihydroxo-bridged structure [55], it is possible that the coupling constant was actually determined for hydroxo-methemerythrin (methemerythrin at pH 8 or above [59]), for which the absorption spectrum indicates a  $\mu$ -oxo- rather than a  $\mu$ -dihydroxo- formulation [3,19].

An overall summary view of the proposed structures for the iron sites of the various states of hemerythrin and of the mechanisms for interconversions between them is shown in Fig. 19. The ligands from the protein have been chosen (somewhat arbitrarily) to be those proposed by Hendrickson et al. [12] from the X-ray structure of azidometmyohemerythrin. The dioxygen and azide ligands are proposed to be coordinated to the iron atom whose His residues, 73 and 101, project from the C and D helices, respectively, since this iron atom is nearer to Trp 97, a residue which may be perturbed upon thiocyanate binding [40].

It is also possible to fit a di-bridged oxyhemerythrin structure into the format of Fig. 19. It should be noted that the non-equivalent environments

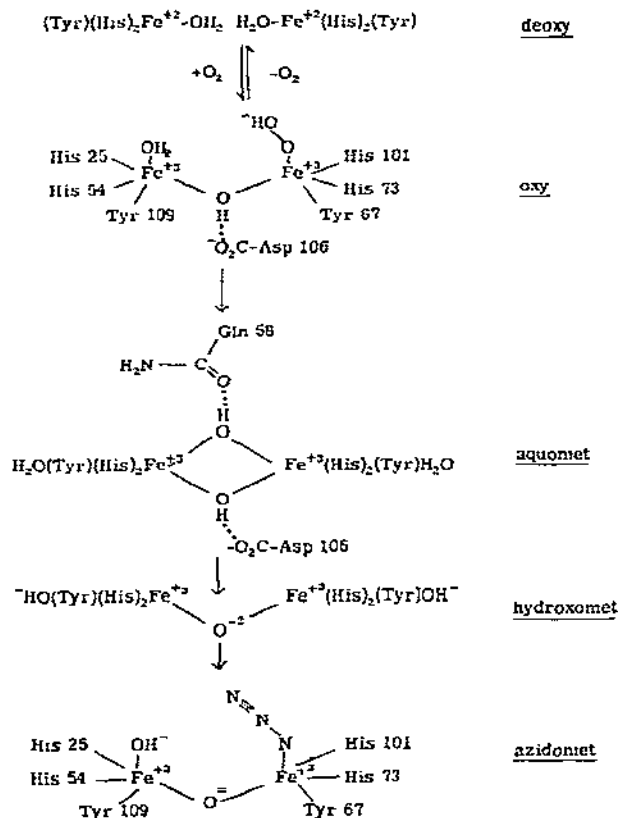
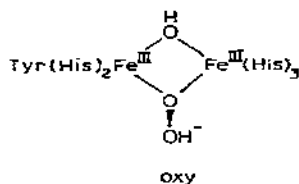


Fig. 19. Proposed structures and mechanisms of interconversion between various states of hemerythrin.

for the iron atoms, seen in Mössbauer spectra, and the absence of an Fe—O peak that is sensitive to  $\text{H}_2^{18}\text{O}$  in resonance Raman spectra, may mean that the structure of oxyhemerythrin differs from that of azidomethemerythrin to the extent that dioxygen bridges the two iron atoms. In this case, the X-ray structure of Stenkamp et al. [33] and non-equivalent environments of the O atoms point to the structure



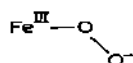
Hydroperoxo structures of this type are known for binuclear cobalt complexes in aqueous acid [60]. Such a structure for oxyhemerythrin could

easily be substituted into the preceding scheme for interconversions between the various states of hemerythrin.

#### E. COMPARISON OF THE OXYGEN BINDING SITES OF HEMERYTHRIN AND HEMOGLOBIN

The problem of reversible oxygen complexation in biological systems has been solved in the case of hemoglobin by means of a mononuclear iron—dioxygen complex and in the case of hemerythrin in terms of a binuclear iron—dioxygen complex. By comparison with frequencies of model compounds [38,39], vibrational spectroscopy has confirmed that dioxygen is reduced when bound to either protein, to a formally superoxide state in the case of hemoglobin [61] and to a formally peroxide state in the case of hemerythrin [36].

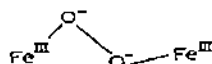
Also on the basis of model compounds, the mononuclear superoxo complex of hemoglobin has generally been considered to have the end-on geometry first proposed by Pauling [62]



An X-ray structure of the  $\text{FeO}_2$  "picket fence" compound tends to support this picture [63].

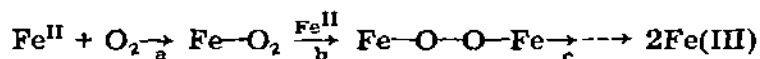
Difference IR spectroscopy shows that oxyhemoglobin contains a band at  $1107\text{ cm}^{-1}$  [61] supporting the end-on superoxo formulation. Difference IR investigations have also been attempted on Fe and Co "picket fence" porphyrins using  $^{16}\text{O}^{18}\text{O}$  [64], but overlapping porphyrin vibrational modes make interpretation of the spectra difficult. Resonance Raman spectra of oxyhemoglobin show no band in the  $1100\text{ cm}^{-1}$  region that can be associated with an O—O stretch, but a weak band does appear at  $567\text{ cm}^{-1}$  which is sensitive to  $^{18}\text{O}_2$  and which has been assigned to the Fe—O stretch of bound dioxygen [65]. An investigation of this region of the spectrum using  $^{16}\text{O}^{18}\text{O}$  could provide evidence for or against an end-on geometry.

The frequencies for  $\nu_{\text{OO}}$  and  $\nu_{\text{FeO}}$  of hemerythrin at  $844\text{ cm}^{-1}$  and  $504\text{ cm}^{-1}$ , respectively, when compared to those of hemoglobin at  $1107\text{ cm}^{-1}$  and  $567\text{ cm}^{-1}$  indicate that much more electron density has been transferred to the antibonding  $\pi^*$  orbitals of dioxygen upon binding by hemerythrin than by hemoglobin. The extra electron transferred in hemerythrin comes from the binuclear rather than mononuclear iron site. From a comparison of model compounds [38,39], the geometry of the binuclear peroxo complex of hemerythrin most reasonably to be expected is

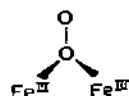


because nearly all known binuclear metal peroxo compounds manifest this structure. However, unlike the case with hemoglobin, no model compounds

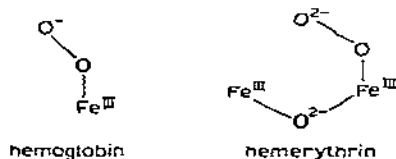
using binuclear iron have yet been characterized adequately to establish that dioxygen can be reversibly reduced to peroxide. In fact, elaborate measures have been used to sterically prevent access of dioxygen to two iron atoms [63,66], i.e. to prevent step b in proposed mechanisms [21,67] leading to irreversible autoxidation of Fe(II) salts



It is possible that step c rather than step b is prevented in hemerythrin. In this case the structure proposed by Stenkamp et al. [33] and non-equivalent O atom environments suggest that the  $\text{Fe}_2\text{O}_2$  moiety of oxyhemerythrin has the structure



An alternative explanation is that step b is also prevented in hemerythrin by limitation of dioxygen access to only one of the iron atoms. The second iron atom then provides the extra electron needed to stabilize  $\text{Fe}^{\text{III}}-\text{O}_2^-$  through a  $\mu$ -oxo or  $\mu$ -hydroxo bridge (whose O atom comes from water) even though that Fe is sequestered away from direct access to dioxygen. Thus, since the O atoms of dioxygen in oxyhemerythrin are in non-equivalent positions, their steric disposition may have the same end-on geometry as in hemoglobin



Since two-electron reverse transfer is necessary for deoxygenation of hemerythrin compared to one-electron transfer for hemoglobin, it has been suggested [39] that the increased oxygen affinity of hemerythrin is due to its reduced "off-rate" compared to that of hemoglobin. The measured "off-rate" for hemerythrin is  $51 \pm 5 \text{ s}^{-1}$  [69], which is in the range of  $10\text{--}60 \text{ s}^{-1}$  measured for dissociation of the first oxygen from hemoglobin. However, dissociation of the remaining oxygens from hemoglobin may occur with much higher velocities [70].

For both hemerythrin and hemoglobin, it is apparent that a molecular structure has been developed that can provide the delicate balance of kinetic and thermodynamic factors necessary to stabilize reversible oxygenation as opposed to irreversible oxidation.

#### ACKNOWLEDGMENT

This investigation was supported in part by the National Heart and Lung Institute (Grant No. HL-08299) of the United States Public Health Service.



## REFERENCES

- 1 J. Bonaventura, C. Bonaventura and B. Sullivan, in F. Jöbsis (Ed.), *Oxygen and Physiological Function*, Professional Information Library, Dallas, Texas, in press.
- 2 I.M. Klotz, G.L. Klippenstein and W.A. Hendrickson, *Science*, 192 (1976) 335.
- 3 K. Garbett, D.W. Darnall, I.M. Klotz and R.J.P. Williams, *Arch. Biochem. Biophys.*, 135 (1969) 419.
- 4 M.Y. Okamura and I.M. Klotz, in G.L. Eichhorn (Ed.), *Inorganic Biochemistry*, Elsevier, New York, 1973, pp. 320-343.
- 5 H.A. De Phillips, Jr., *Arch. Biochem. Biophys.*, 144 (1971) 122.
- 6 C.P. Mangum and M. Kondon, *Comp. Biochem. Physiol.*, 50 (1975) 777.
- 7 A. Rossi-Fanelli, E. Antonini and A. Caputo, *Advan. Prot. Chem.*, 19 (1964) 73.
- 8 I.M. Klotz and S. Keresztes-Nagy, *Biochemistry*, 2 (1963) 445.
- 9 G.L. Klippenstein, D.A. Van Ripper and E.A. Oosterum, *J. Biol. Chem.*, 247 (1972) 5959.
- 10 K.B. Ward, W.A. Hendrickson and G.L. Klippenstein, *Nature (London)*, 257 (1975) 818.
- 11 R.E. Stenkamp, L.C. Sieker, L.H. Jensen and J.S. Loehr, *J. Mol. Biol.*, 100 (1976) 23.
- 12 W.A. Hendrickson, G.L. Klippenstein and K.B. Ward, *Proc. Nat. Acad. Sci. U.S.A.*, 72 (1975) 2160.
- 13 D.W. Darnall, K. Garbett, I.M. Klotz, S. Aktipis and S. Keresztes-Nagy, *Arch. Biochem. Biophys.*, 133 (1969) 103.
- 14 G.L. Klippenstein, J.W. Holleman and I.M. Klotz, *Biochemistry*, 7 (1968) 3868.
- 15 G.L. Klippenstein, *Biochemistry*, 11 (1972) 372.
- 16 I.M. Klotz, T.A. Klotz and H.A. Fiess, *Arch. Biochem. Biophys.*, 68 (1957) 284.
- 17 E. Boeri and A. Ghirelli-Magaldi, *Biochim. Biophys. Acta*, 23 (1957) 465.
- 18 I.M. Klotz and T.A. Klotz, *Science*, 121 (1955) 477.
- 19 S. Keresztes-Nagy and I.M. Klotz, *Biochemistry*, 4 (1965) 919.
- 20 M.H. Klapper and I.M. Klotz, *Biochemistry*, 7 (1968) 223.
- 21 K.S. Murray, *Coordin. Chem. Rev.*, 12 (1974) 1, and refs. cited therein.
- 22 H.B. Gray and H.J. Schugar, in G.L. Eichhorn (Ed.), *Inorganic Biochemistry*, Elsevier, New York, 1973, pp. 102-118.
- 23 J.W. Dawson, H.B. Gray, H.E. Hoening, G.R. Rossmann, J.M. Schredder and R.H. Wang, *Biochemistry*, 11 (1972) 461.
- 24 T.H. Moss, C. Moleski and J.L. York, *Biochemistry*, 10 (1971) 840.
- 25 J.L. York and A.J. Bearden, *Biochemistry*, 9 (1970) 4549.
- 26 M.Y. Okamura, I.M. Klotz, C.E. Johnson, M.R.C. Winter and R.J.P. Williams, *Biochemistry*, 8 (1969) 1951.
- 27 K. Garbett, C.E. Johnson, I.M. Klotz, M.Y. Okamura and R.J.P. Williams, *Arch. Biochem. Biophys.*, 142 (1971) 574.
- 28 G.L. Klippenstein, *Biochem. Biophys. Res. Commun.*, 49 (1972) 1474.
- 29 J.A. Morrissey, Ph.D. Dissertation, University of New Hampshire, 1971.
- 30 C.C. Fan and J.L. York, *Biochem. Biophys. Res. Commun.*, 47 (1972) 472.
- 31 R.M. Rill and I.M. Klotz, *Arch. Biochem. Biophys.*, 136 (1970) 507.
- 32 G.L. Klippenstein, J.L. Cote and S.E. Ludlam, *Biochemistry*, 15 (1976) 1128.
- 33 R.E. Stenkamp, L.C. Sieker and L.H. Jensen, *Proc. Nat. Acad. Sci. U.S.A.*, 73 (1976) 349.
- 34 L.H. Jensen, personal communication.
- 35 A.Y. Hirakawa and M. Tsuboi, *Science*, 188 (1975) 359; E.S. Yeung, M. Heiling and G.J. Small, *Spectrochim. Acta*, Part A, 31 (1975) 1921.
- 36 J.B.R. Dunn, D.F. Shriver and I.M. Klotz, *Proc. Nat. Acad. Sci. U.S.A.*, 70 (1973) 2582.
- 37 J.B.R. Dunn, D.F. Shriver and I.M. Klotz, *Biochemistry*, 14 (1975) 2689.

- 38 L. Vaska, *Accounts Chem. Res.*, 9 (1976) 175.
- 39 G. McLendon and A.E. Martell, *Coordin. Chem. Rev.*, 19 (1976) 1.
- 40 D.M. Kurtz, Jr., Ph.D. Dissertation, Northwestern University (1977).
- 41 D.M. Kurtz, Jr., D.F. Shriver and I.M. Klotz, *J. Am. Chem. Soc.*, 98 (1976) 5033.
- 42 J. Lewis, R.S. Nyholm and P.W. Smith, *J. Chem. Soc.*, (1961) 4590.
- 43 L.H. Jensen, *Annu. Rev. Biochem.*, 43 (1974) 461.
- 44 R.A. Bailey, *Coordin. Chem. Rev.*, 6 (1971) 407.
- 45 P.G. David, *J. Inorg. Nucl. Chem.*, 35 (1973) 1463.
- 46 E.B. Wilson, J.C. Decius and P.C. Cross, *Molecular Vibrations*, McGraw-Hill, New York, 1955.
- 47 J.H. Schachtschneider, *Vibrational Analysis of Polyatomic Molecules*, V. FORTRAN IV Programs for Setting Up the Vibrational Secular Equation, Project No. 31450, Technical Rpt. No. 231-234, Shell Development Co., Emeryville, California, 1966.
- 48 J.H. Schachtschneider, *Vibrational Analysis of Polyatomic Molecules*, VI. FORTRAN IV Programs for Solving the Vibrational Secular Equation and for the Least Squares Refinement of Force Constants, Project No. 31450, Technical Rpt. No. 57-65, Shell Development Co., Emeryville, California, 1966.
- 49 D.R. Meloon and R.G. Wilkins, *Biochemistry*, 15 (1976) 1284.
- 50 D. Samuel, in O. Hayaishi (Ed.), *The Oxygenases*, Academic Press, New York, 1962, pp. 45-58.
- 51 B.P. Gaber, V. Miskowski and T.G. Spiro, *J. Am. Chem. Soc.*, 96 (1974) 6868.
- 52 R.M. Wing and L.P. Callahan, *Inorg. Chem.*, 8 (1969) 871.
- 53 J. San Fillipo, Jr., R.L. Grayson and H.J. Sniadoch, *Inorg. Chem.*, 15 (1976) 269.
- 54 J.B.R. Dunn, T.M. Loehr, J.S. Loehr, A.W. Addison and R.E. Bruce, *Biochemistry*, 16 (1977) 1743.
- 55 J.A. Thich, C.C. Ou, D. Powers, B. Vasilou, D. Mastropaolo, J.A. Potenza and H.J. Schugar, *J. Am. Chem. Soc.*, 98 (1976) 1425 and refs. cited therein.
- 56 G. McLendon, R.J. Motekaitis and A.E. Martell, *Inorg. Chem.*, 15 (1976) 2306.
- 57 C. Walling, M. Kurz and H.J. Schugar, *Inorg. Chem.*, 9 (1970) 931.
- 58 J.B.R. Dunn, personal communication.
- 59 K. Garbett, D.W. Darnall and I.M. Klotz, *Arch. Biochem. Biophys.*, 142 (1971) 471.
- 60 U. Thewalt and R. Marsh, *J. Am. Chem. Soc.*, 89 (1967) 6364.
- 61 C.H. Barlow, J.C. Maxwell, W.J. Wallace and W.S. Caughey, *Biochem. Biophys. Res. Commun.*, 55 (1973) 91.
- 62 L. Pauling, *Nature (London)*, 203 (1964) 182.
- 63 J.P. Collman, R. Gagne, C.A. Reed, W. Robinson and G. Radley, *Proc. Nat. Acad. Sci. U.S.A.*, 71 (1974) 1326.
- 64 J.P. Collman, J.I. Braumann, T.R. Halbert and K.S. Suslick, *Proc. Nat. Acad. Sci. U.S.A.*, 73 (1976) 3333.
- 65 H. Brunner, *Naturwissenschaften*, 61 (1974) 129.
- 66 J. Amlog, J.E. Baldwin and J. Huff, *J. Am. Chem. Soc.*, 97 (1975) 227.
- 67 I.A. Cohen and W.S. Caughey, *Biochemistry*, 7 (1968) 636; J.O. Alben, W.H. Fuchsmann, C.A. Beaudreau and W.S. Caughey, *Biochemistry*, 7 (1968) 624; G.S. Hammond and C.-H.S. Wu, *Advan. Chem. Ser.*, 77 (1968) 186.
- 68 D.M. Kurtz, Jr., D.F. Shriver and I.M. Klotz, unpublished observations.
- 69 D.J.A. de Waal and R.G. Wilkins, *J. Biol. Chem.*, 251 (1976) 2339.
- 70 E. Antonini and M. Brunori, *Hemoglobin and Myoglobin in their Reaction with Ligands*, North Holland, Amsterdam, 1971, pp. 256-257.